

AD-A034 284

AIR FORCE INST OF TECH WRIGHT-PATTERSON AFB OHIO
ANALYSIS OF THE SUN PUMPED LASER CONE OPTICS.(U)
SEP 76 P M TOWLES

SCH--ETC F/6 20/5

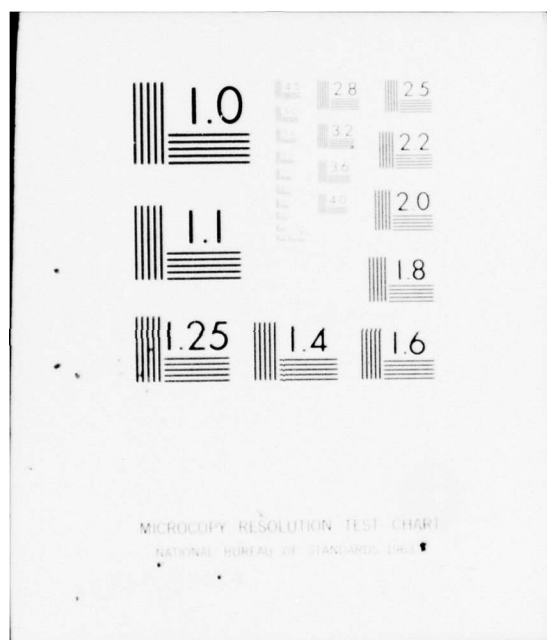
UNCLASSIFIED

SEP/PM/76-11

NL

1 OF 1
AD
A034284





ADA034284



1
B.S.



UNITED STATES AIR FORCE
AIR UNIVERSITY
AIR FORCE INSTITUTE OF TECHNOLOGY
Wright-Patterson Air Force Base, Ohio

DISTRIBUTION STATEMENT A
Approved for public release
Distribution Unlimited

D D C
RECEIVED
JAN 10 1977
RECEIVED
A

⑥ ANALYSIS OF THE SUN PUMPED
LASER CONE OPTICS.

⑨ Master's THESIS,

⑭ GEP/PH/76-11

⑩ Perry M. Towles
Capt USAF

⑪ Sep 76

⑫ 60p.

Michael D D C
RECEIVED
JAN 10 1977
RECEIVED
A ✓

Approved for public release; distribution unlimited

012 225
bpg

ANALYSIS OF THE SUN PUMPED

LASER CONE OPTICS

THESIS

Presented to the Faculty of the School of Engineering
of the Air Force Institute of Technology

Air University

in Partial Fulfillment of the
Requirements for the Degree of
Master of Science

by

Perry M. Towles, B.S.

Capt USAF

Graduate Engineering Physics

September 1976

Approved for public release; distribution unlimited

REVISION 100	
OTIS	W. H. Dwyer <input checked="" type="checkbox"/>
ENG	W. H. Dwyer <input type="checkbox"/>
QUALIFICATION	<input type="checkbox"/>
DISTRIBUTION, AVAILABILITY CODES	
Dist.	Avail. and/or SPECIAL
A	

Preface

This report is an attempt to help Space and Missiles Systems Organization (SAMSO) solve a problem with a Sun Pumped Laser. This report does not contain all the work accomplished in obtaining the results. Some third order aberration theory analysis was accomplished to give me some insights into the spherical aberration problems in the lens.

I wish to express my gratitude to my thesis advisor, Dr. Kaplan and the SAMSO sponsor, Capt. Kennedy. They provided me with a continuous flow of information that was not only beneficial, but also kept me from going down erroneous paths.

I also wish to especially acknowledge my gratitude and indebtedness to my wife for not only typing this report, but also for her support and encouragement during my thesis research.

Perry M. Towles

Contents

Preface	ii
List of Figures	iv
List of Tables	v
Abstract	vi
I. Introduction	1
II. System Description	7
Gaussian Approximation	10
III. Condensing Cone Theory	12
IV. Snell's Law Ray Trace Derivation	16
Ray Converging Toward the Optic Axis	17
Ray Diverging From the Optic Axis	19
Refraction of a Ray at a Planar Surface	21
V. Skew Ray Analysis	24
VI. Results and Conclusions	27
Bibliography	37
Appendix A: Entrance Pupil Calculation	38
Appendix B: Power "Weight Factor" Derivation for Radial Zones	40
Appendix C: Derivation of the "Azimuth Zone Power Factors" Used to Calculate the Power Distribution Out of the Condensing Cone by Exit Angle	43

List of Figures

<u>Figure</u>		<u>Page</u>
1	Sun Pumped Laser	2
2	Solar Power Collected as a Function of Normalized Primary Mirror Area	4
3	Cassegrainian System	7
4	Cross Sectional View of Cone Lens and Condenser Cone	9
5	Condenser Cone and Reference Circle	13
6	Geometrical Ray Tracing in a Simple Cone	13
7	Reference Circle Zones	14
8	Ray Converging Towards the Optic Axis	18
9	Ray Diverging From the Optic Axis	20
10	Refraction at a Planar Surface	22
11	Through Power (for 5% loss per bounce) vs.. Distance Between Relay Lens and Cone Lens	28
12	Primary Mirror Radius vs. Through Power at 10.8 cm	32
13	Primary Mirror Radius vs. Through Power at 12.2 cm	33
14	Primary Mirror Radius vs. Through Power at 13.0 cm	34
15	Solar Image and Entrance Pupil Image Radial Zones	41
16	Ray Intersect Angles for Condenser Cone Exit	44
17	Ray Intersect Angle for Converging Ray (\bar{B})	46

List of Tables

<u>Table</u>		<u>Page</u>
I	Component Characteristics and Spacing	8
II	Summary of Solar Information	10
III	Table of Skew Ray Characteristics	25
IV	Primary Mirror Radius Equated to Normalized Mirror Area	27
V	Power Loss for 5%, 15%, and 25% Loss Per Reflection . .	31
VI	Azimuth Zone Power Factors for 9.9, 12.2 and 13.2 cm Seperation	35
VII	System Elements and Parameters Used in Entrance Pupil Calculation	39
VIII	Azimuth Zone Power Factors for Different Distances Between the Relay Lens and the Cone Lens	49

Abstract

A meridional ray analysis is accomplished on the solar energy collector part of a sun pumped laser. A Gaussian approximation is completed and shows a solar image 0.57 inches in diameter is located 3.81 cm from the end of the laser rod. The image is inside the laser cavity.

The peak in meridional ray through power is found when there is a separation distance of 12.2 cm between the relay lens and the cone lens, condensing cone element.

For 200 watts available at the primary mirror of the Cassegrainian System, it is found that only about 150 watts is furnished to the cone lens for through put. Only about 66% of the available 150 watts is collected by the cone lens and channelled to the laser rod by the condensing cone.

The last is found by a skew ray analysis of some rays coming from the outer radial part of the primary mirror. These rays are traversing the system all the way to the cone lens, but are diverging before entering the lens and therefore not being collected by the condenser cone.

An analysis is made of the exit angle of the power traversing the condenser cone. The analysis was made so that an AR coating of the appropriate material and thickness could be put on the laser rod for maximum collection of the solar energy wavelengths used in pumping the Nd:YAG laser rod.

I. INTRODUCTION

In the early 1980's, another communications satellite will be put into orbit. This satellite will be different from the previous ones in that one of the transmitters will be a Sun Pumped Nd:YAG Laser. The Nd:YAG laser rod is usually side pumped by a lamp or light emitting diodes, which have a very short lifetime compared to the needs of an operating communications satellite. The requirement existed to find a method of pumping the laser that would not be depleted in a short time, compared to the satellite operating lifetime. The old method of extending the operating lifetime of the laser was to utilize rotating banks of argon lamps, where the bank would rotate and a new pump lamp would be used when the old lamp had burned out.

The use of rotating banks of pump lamps only extends the useable lifetime of the laser a small amount, compared to the total satellite system lifetime. Therefore, a method of pumping had to be found which would not limit the useful lifetime of the laser. The feasibility of pumping a Nd:YAG laser rod by focusing the sun's energy on the rod has been looked at for over ten years. In 1964, G. R. Simpson (Ref. 1) achieved operation of a sun pumped laser with a Nd: Glass rod as the lasing material. Then in 1966, C. G. Young (Ref. 2) developed a sun pumped Nd:YAG Laser that operated continuous wave (CW) with approximately one watt of output.

In the early 1970's, SAMSO contracted to have a sun pumped Nd:YAG Laser developed for use in a communications satellite. The early

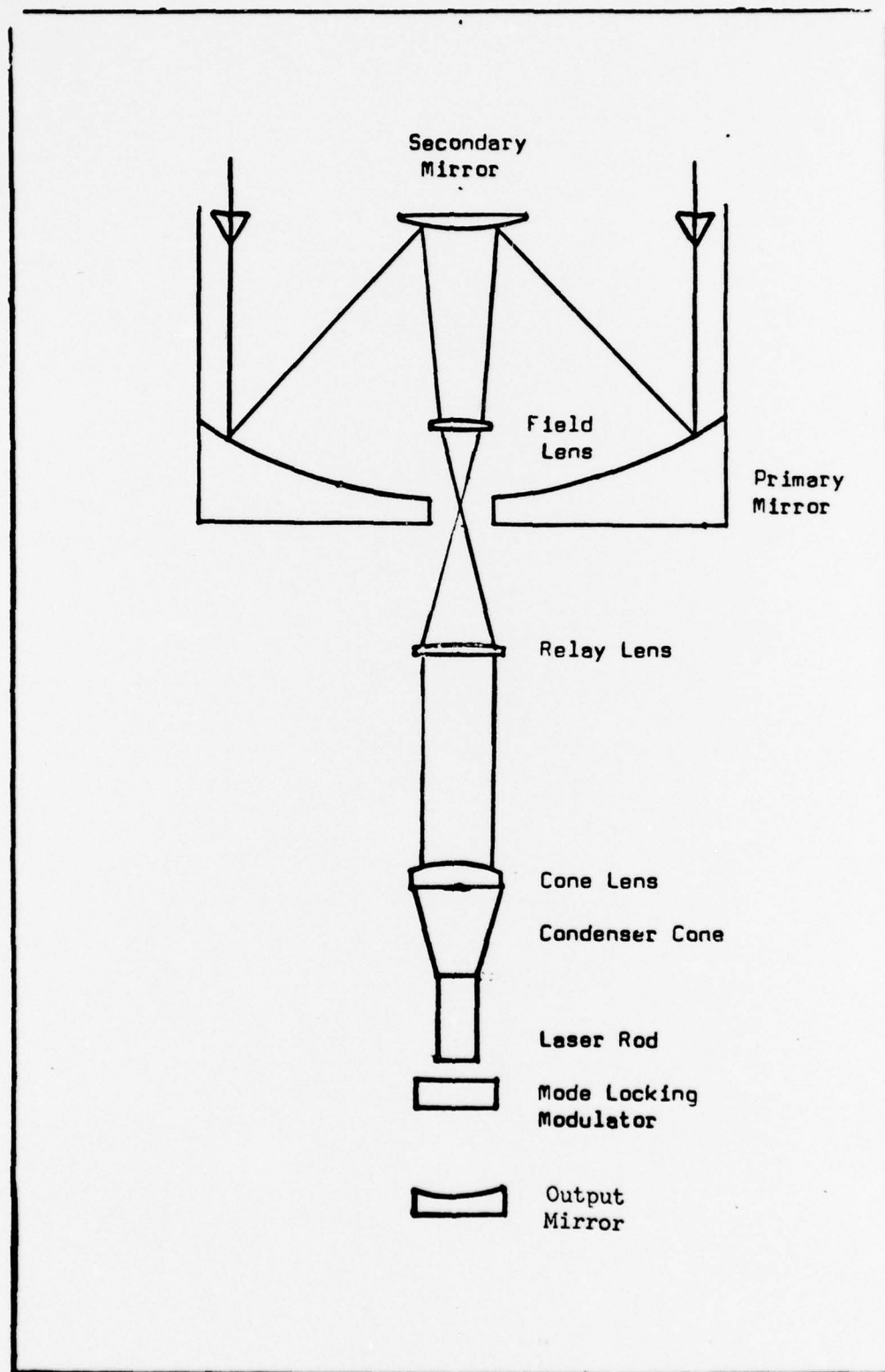


Fig. 1 - Sun Pumped Laser (From Ref. 4)
(Not to Scale)

development produced a design as shown in Fig. 1. It was discovered during testing of the system to determine the through power (through power is defined as the power that exits the end of the condensing cone (Fig. 1) attached to the laser rod) that only about 40% of the power available from the relay lens was exiting the condenser cone, for a aperature ratio which is defined as the area of the primary mirror (Fig. 1) used versus the total area of the primary mirror available, of 1. From Fig. 2 it is seen that as the area of the primary mirror is decreased the percentage of through power versus available power increases. The reason for this is that as the primary mirror area is decreased, a higher percentage of the available solar rays approach the paraxial approximation. An analysis of the system to determine the reason for the low percentage of through power would be of assistance to SAMSO. This would enable SAMSO to try different corrective methods for increasing the through power available from the Sun Pumped Nd:YAG Laser. The two most likely candidates contributing to the power loss were excessive spherical aberration by the Relay and Cone Lens, and the inability of a skew ray to propagate through the system.

There are three terms which will be used frequently throughout this report, they are Meridional Rays, Skew Rays, and Spherical Aberration. Following is a short definition of each of these terms and the conditions for their use.

A Meridional ray is defined as a ray that lies in a plane containing the optic axis and the initial object point. In tracing a meridional ray through an optical system the ray will always stay in the plane containing the object point and the optic axis. Therefore, a Meridional ray analysis is basically a two dimensional analysis of the ray path through the system.

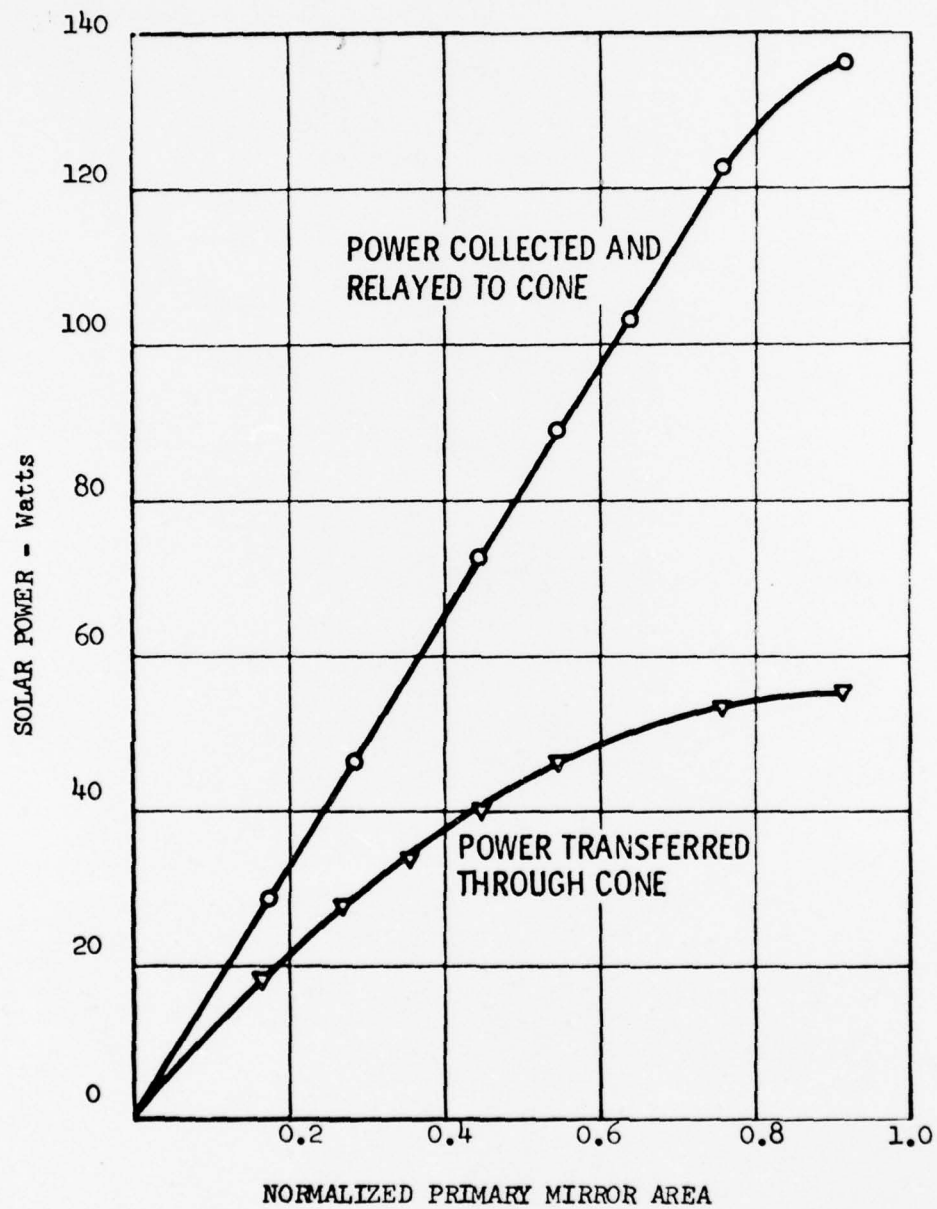


Fig. 2 - Solar Power Collected as a Function of Normalized Primary Mirror Area (From Ref. 4)

A Skew Ray is defined as non-meridional ray. In doing a skew ray analysis of an optical system a three dimensional analysis is mandatory. Therefore, a skew ray analysis is a very detailed process and requires more effort than other types of analysis.

Spherical Aberration is defined as a type of monochromatic aberration in which an object on the optic axis is not focused at a unique point by a lens. All lenses with a spherical contour on their outer surfaces have a certain amount of spherical aberration.

Since a meridional ray analysis will show the effect of spherical aberration and is easier to accomplish, it was decided to determine the through power loss due to spherical aberration in the relay and cone lens. Once this has been determined, the assumption could be made that the through power lost by the system not due to spherical aberration is attributable to the skew rays not being able to get to or through the cone lens and/or condenser cone. A quick analysis could then be made of several of the skew ray going through the system to determine if they do propagate to the exit of the condenser cone.

The observed phenomena of the through power percentage getting larger as the presented aperture area was reduced also was looked at. This was accomplished for several different configuration of the Sun Pumped Laser System. The analysis was accomplished using only meridional rays. The difference in calculated versus measured through power for the configurations looked at would also show the amount of skew ray loss through the system for different primary mirror diameters.

With the power collected by the sun pumped laser being channeled to the end of the laser rod by a condenser cone, the problem of determining

the angular distribution at which the maximum power is incident on the laser rod was investigated.

In the usual method of side-pumping a Nd:YAG laser rod the ends are cut flat or cut at the Brewster's angle if polarization is important. If the laser rod is to be end pumped then the system's ability to collect the maximum amount of power incident on the laser rod end could be enhanced if an analysis would show the angles at which most of the power is incident. Then an anti-reflection (AR) coating could be put on the end of the laser rod increasing the amount of incident power transmitted to the rod. Appendix C shows the method used in calculating the power out by exit angle.

II. System Description

The Primary Mirror and Secondary Mirror (Fig. 1) of the sun pumped laser form a Cassegrainian System. The term "Cassegrainian System" now applies to any telescope system consisting of a concave primary and a convex secondary mirror, which is different than the system originally proposed by Cassegrain, of a paraboloidal primary with a hyperboloidal secondary. Most Cassegrainian systems (Fig. 3) are characterized (Ref. 3, page 19-9) by the ratio of the secondary mirror image distance ($F2$ to $M2$) versus the distance of the primary mirror focal point to the secondary mirror ($F1$ to $M2$). The ratio for this system is 7.16.

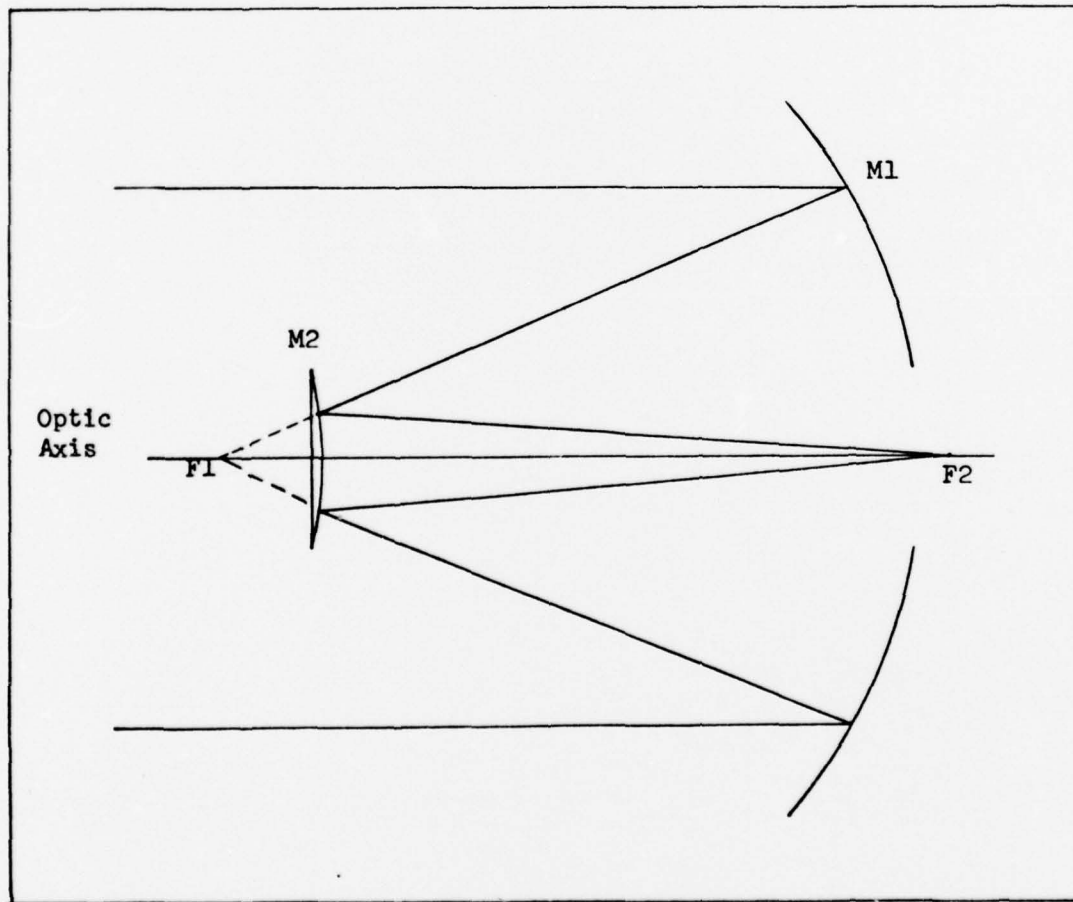


Fig. 3 Cassegrainian System

Table I lists all the components of the sun pumped laser and the characteristics of each component. Table I also shows the spacing between components. Reference is made to Figure 1 for the placement of the individual component in the system.

Table I			
Component Characteristics and Spacing			
	<u>Focal Length</u>	<u>Diameter</u>	<u>Material</u>
Primary Mirror	+35.74"	24.0"	Aluminized Coating
Distance between Primary and Secondary is 32.72"			
Secondary Mirror	-3.51"	3.0"	Silver Coating
Distance between Secondary Mirror and Field Lens is 20.72"			
Field Lens	+10.6"	3.0"	Quartz (n=1.44)
Distance between Field Lens and Relay Lens is 19.0"			
Relay Lens	+4.0"	3.0"	Crown Glass (n=1.51)
Distance between Relay Lens and Cone Lens is 5.0"			
Cone Lens	+1.5"	1.0"	Bk7 (n=1.45)
The back surface of the cone lens is against the front surface of the Condenser Cone (see Fig. 4).			

The Field Lens (see Fig. 1), which is -12" from the vertex of the primary mirror has a 10.6" focal length and is 3" in diameter. It has a single layer of MgF as an AR coating and an index of refraction of 1.44. It is a symmetrical bi-convex lens, has a radius of curvature of approx 22.70 centi-

meters and is approximately 0.66 centimeters thick at its vertex.

The Relay Lens (see Fig. 1) is located +7" from the primary and is a plano convex lens. It is 3" in diameter and has a 4" focal length. The Relay Lens has a single layer AR coating of MgF, an index of refraction of 1.51 and a thickness of 1.669 centimeters.

The Cone Lens is located +12 inches from the Primary Mirror and is 5" from the Relay Lens. It is a one inch diameter plano convex lens of 1.5 inches focal length, an index of refraction of 1.45 and a radius of curvature of 1.7145 cm. on its front surface. The Cone Lens has a thickness of 0.56 cm. at its vertex, a single layer of MgF AR coating, and a circular laser mirror (100% reflectivity at 1.06 microns and 80% transmission at the solar energy wavelengths) of 2.5 mm radius on its planar surface.

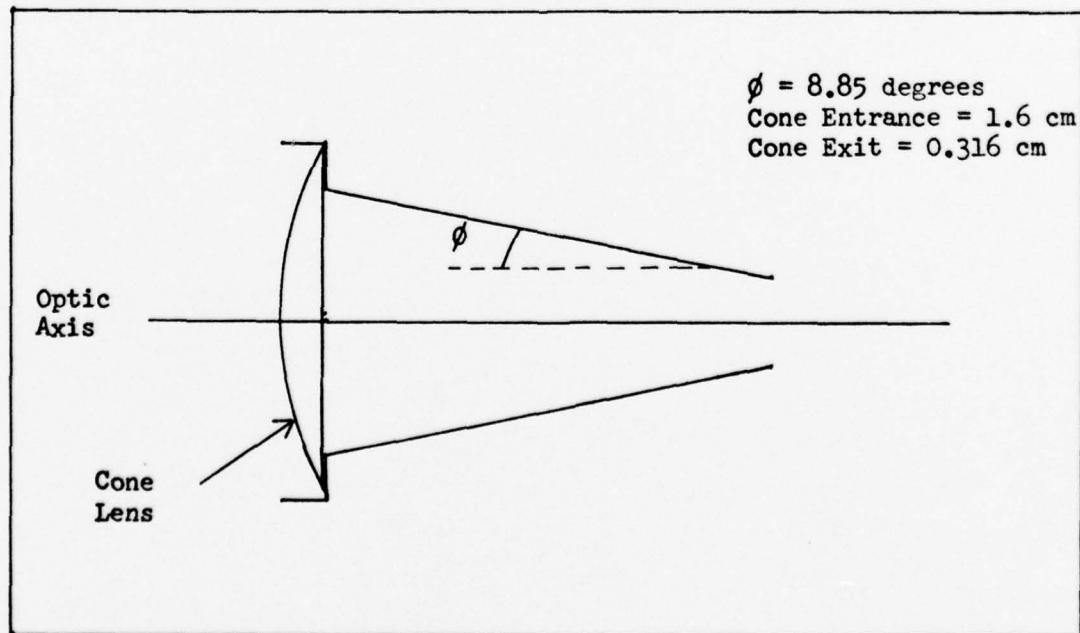


Fig. 4 - Cross Sectional View of Cone Lens and Condenser Cone (Not to Scale)

The rear surface (plano surface) of the Cone Lens is against the entrance of the Condensing Cone. The Condensing Cone (Figure 4) has a circular entrance opening of 0.80 cm. radius and a circular exit opening of 1.58 mm. The Condenser Cone has a cone angle of 8.85 degrees with the optic axis and is 4.119 cm. in length. The Condensing Cone was fabricated (Ref. 4) by the electroforming process using a conical stainless steel mandrel. A layer of silver is first electrodeposited onto the mandrel and then a thick layer of copper is electroformed over the silver.

Table II

Summary of Solar Information

1. Solar intensity at sea level-----0.068 watts/cm²
(at 5000 Angstroms)
 2. Distance of Sun from the Earth-----9.29 x 10⁷ miles
 3. Diameter of Sun-----8.64 x 10⁵ miles
 4. Angle subtended by the Sun-----0.5 degrees
-

A Gaussian analysis can now be done using the information given in Tables I and II and the characteristics of the imaging part of the sun pumped laser.

Gaussian Approximation

1. Primary Mirror - Using the Lensmakers Equation (Eq. 1)

$$1/S_o + 1/S_i = 1/F \quad (1)$$

an object distance of 9.29 x 10⁷ miles (1.49 x 10¹³ cm.) and a focal length of 90.77 cm. we get a solar image at 90.77 cm. Then we can find the image radius from the Magnification Equation (Eq. 2)

$$M = S_i/S_o \quad (2)$$

Plugging in the calculated values, we get a magnification of 6.07×10^{-12} and an image radius of 0.42 cm.

2. Secondary Mirror - The solar image from the primary becomes the virtual object for the secondary and we have an object distance of -7.67 cm. and a focal length of -8.91 cm. Applying Eq. 1 again we get a solar image at 55.11 cm. from the secondary. Using the magnification equation (Eq. 2) again, we get an image radius of 3.01 cm.

3. Field Lens - A virtual object is seen by the Field Lens at 2.48 cm. Applying Eq. 1 for a focal length of 26.92 cm, we get a solar image at 2.27 cm. and an image radius of 2.75 cm.

4. Relay Lens - The solar image from the Field Lens becomes the real object for the Relay Lens. The object distance is 45.99 cm. giving an image at 13.04 cm. from a focal length of 10.16 cm. We get an image size of 0.78 cm. radius.

5. Cone Lens - The Cone Lens see a virtual object at -0.34 cm. With a focal length of 3.81 cm. and using Eq. 1 we get a solar image at 0.31 cm. of 1.43 cm. diameter.

From a Gaussian approximation of the sun pumped laser solar collector there is a solar image 0.56 inches in diameter and the image is located 3.80 cm. in front of the exit opening of the Condenser Cone.

III. Condensing Cone Theory

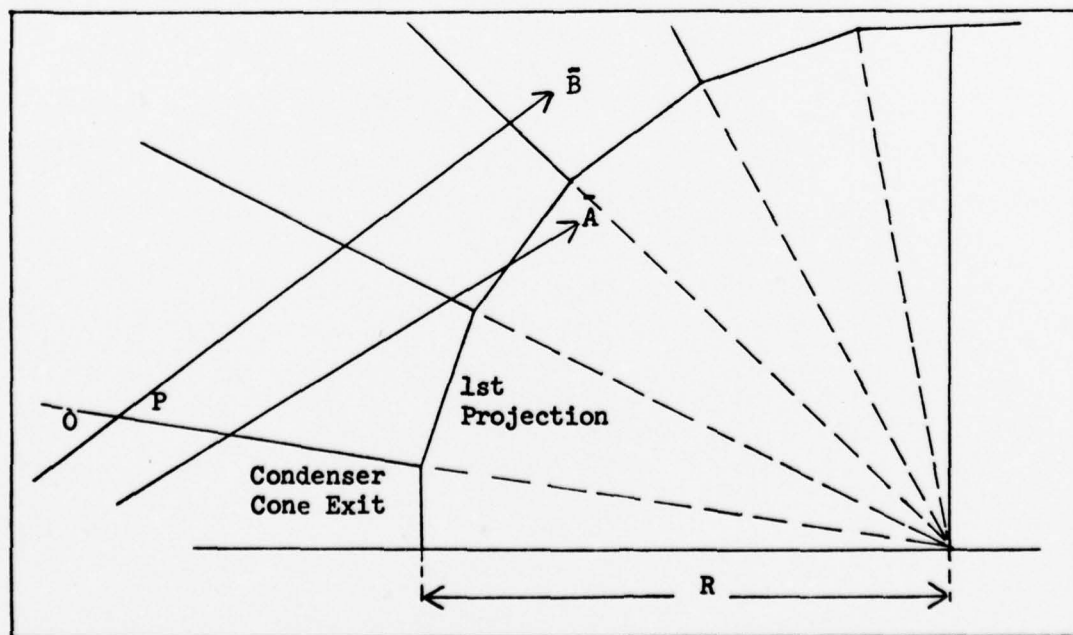
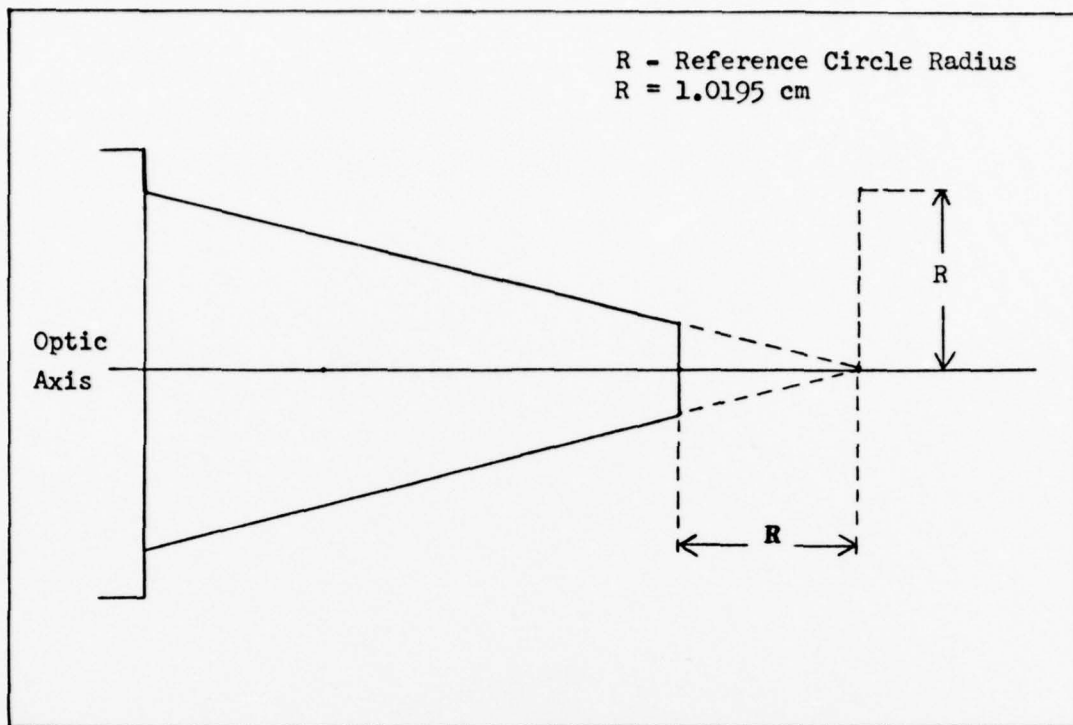
Before an analysis of the system can be made, an understanding of the Condenser Cone and how it channels energy to the laser rod is necessary. From Fig. 1, it is seen that the Condenser Cone is the last element in the solar collector before the laser rod. This makes the efficiency of the system very dependent on the efficiency of the Condenser Cone. Condenser Cone theory and how the energy is channelled through the cone was studied by Donald E. Williamson (Ref. 5) in the early 1950's. The theory used in this analysis is mainly derived from his work.

The type of Condenser Cone used in this system is a right circular cone. A physical description of the cone is given in Section 2 (System Description). Figure 4 is a cross sectional view of the Condenser Cone.

From Fig. 5 it is seen that the exit opening of the cone is normal to the optic axis and a small distance from where the vertex would have been. The distance from the exit opening to the projected vertex of the cone is very important in the analysis of the cone and will be referred to as the radius of the reference circle.

An understanding of the way in which meridional rays are received by a condensing cone at its entrance opening and transmitted to its exit is seen by reference to Fig. 6 and the following theory.

The image space of a Condenser Cone is formed by rotating the cone about one of its reflecting surfaces. A closed polygon will be formed if the reflecting surface is rotated 360 degrees about its vertex. The polygon will have an average radius that is equal to the reference circle radius previously defined. If a ray is then drawn entering the entrance of the Condensing Cone, and the straight line projection of the ray enters the reference circle (Ray A of Fig. 6), the ray will pass through the exit



opening of the cone. The number of bounces the ray will make before exiting the cone can be determined by counting the number of cone wall projections the ray crosses before entering the reference circle. The intersection of the ray with the reference circle does not count as a reflection. The counting of reflections is necessary in determining the remaining energy in a ray since the energy loss per reflection for the copper surface is known. Therefore, if a ray makes a large number of bounces before entering the reference circle its energy will be significantly reduced. If a straight line projection of a ray does not intersect the reference circle (Fig. 6, Ray B), then the ray will suffer a reversal and come back out the entrance opening after the appropriate number of bounces.

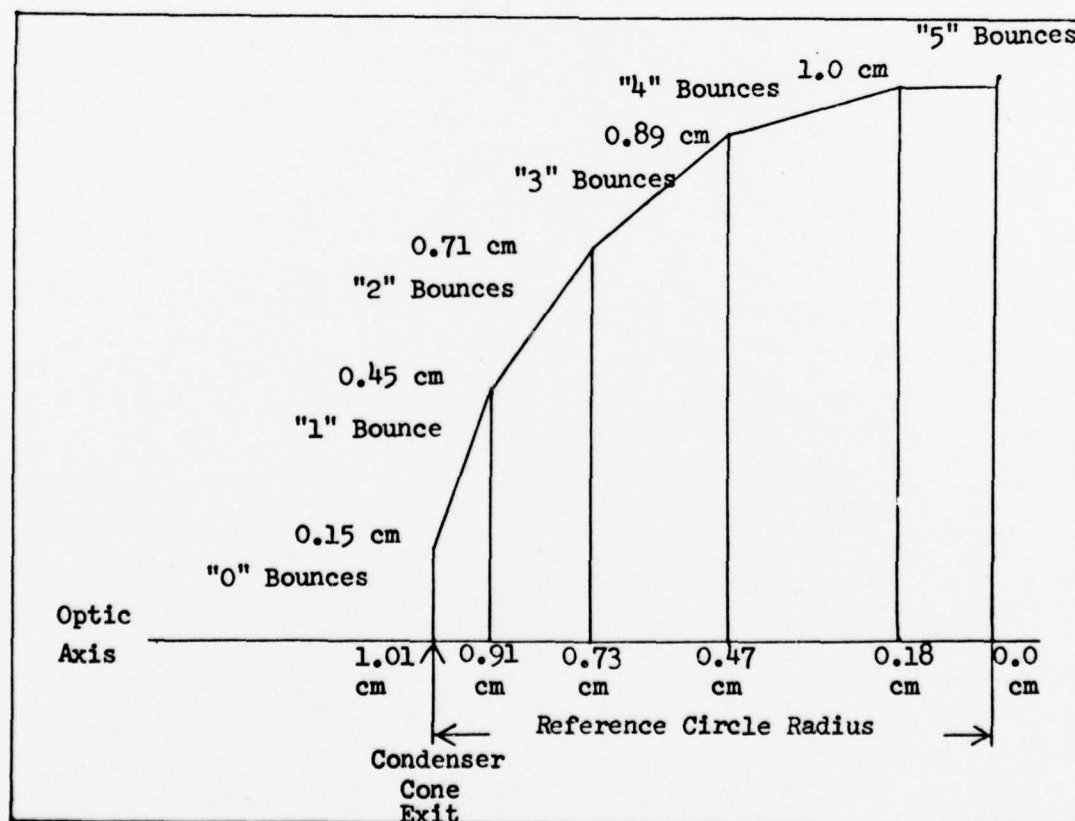


Fig. 7 - Reference Circle Zones

A geometrical analysis and the law of reflection (incident angle equals reflected angle) can be used to show that angle O equals angle P in Fig. 6 and therefore angle P is the same angle as the reflected angle for a ray reflected from the surface.

From Fig. 6 it is seen that the number of bounces the ray makes in exiting the Condensing Cone is a function of the height of a ray above the optic axis (using the straight line projection) at the exit opening of the cone. If the edges of the reference circle rotations are projected so that they intersect the optic axis at normal incidence, as in Fig. 7, then the height of the different bounce zone and their distance along the optic axis from the projected cone vertex can be easily calculated.

In an energy calculation of a ray the only parameters necessary are its height at different points along the optic axis. This calculation can also be used to identify the rays that will reverse their path and not go through the exit opening of the Condensing Cone. Figure 7 shows the heights and distances for the Condensing Cone used in the sun pumped laser.

IV. SNELL'S LAW RAY TRACE DERIVATION

In the design of a computer program to calculate the through power for the solar collector of the sun pumped laser, three assumptions were made. They are:

- a. A real solar image was located 45.99 cm. from the front vertex of the relay lens and was 2.75 cm. in radius. (See Section II for the Gaussian approximation).
- b. The primary mirror was the aperture stop and entrance pupil (See Appendix A) and was imaged at the first principal plane of the relay lens.
- c. Only rays coming from the solar image 46.12 cm. in front of the relay lens and passing through the primary mirror image at the relay lens will pass through the solar collector.

Using these assumptions, rays could be traced through the relay lens, cone lens, and condensing cone and the power loss in each ray could then be calculated. The initial power in each ray was a function of the normalized area of the solar image zone from which it started, times the normalized area of the entrance pupil image zone through which it passed (for derivation of weighting factor and power of each ray zone see Appendix B)..

In following a ray through the solar collector, refraction occurred for three different basic conditions.

- a. Refraction at a convex surface for a ray converging toward the optic axis.
- b. Refraction at a convex surface for a ray coming from the optic axis.
- c. Refraction of a ray at a planar surface.

The Snell's law ray trace equations for the above listed conditions

follow The following nomenclature will be used in the Snell's law ray trace analysis:

- a. R_1 - Radius of curvature of the surface
- b. N_0 - Index of refraction of air
- c. N_1 - Index of refraction of the lens material

All rays are also assumed to travel from left to right for this analysis.

A. Ray Converging Towards the Optic Axis

The method used in tracing a ray through the system for the condition that the ray is converging towards the optic axis when it strikes the surface, is derived from Reference 6, Section 4.9.

Figure 8 shows the condition for this derivation. The following sign convention is used: The distances R_1 , M , and L are positive where they are to the right of the vertex. The angles θ_{AE} and θ_{Al} are positive if the rays making the angles intersect the optic axis to the right of the vertex. The angles ϕ_{1A} and ϕ_{1B} are positive if the rays forming the angles cross the optic axis to the right of C . Also the distance AC is equal to R_1 .

From the Law of Sines for triangle CPB (Fig. 8) we have:

$$\frac{L-R_1}{\sin(\phi_{1A})} = \frac{R_1}{\sin(\theta_{AE})} \quad (3)$$

Therefore

$$\sin(\phi_{1A}) = \frac{(L-R_1)}{R_1} \sin(\theta_{AE}) \quad (4)$$

Using Snell's Law

$$N_1 \sin(\phi_{1B}) = N_0 \sin(\phi_{1A}) \quad (5)$$

It can be seen that

$$\sin(\phi_{1B}) = \frac{N_0}{N_1} \sin(\phi_{1A}) \quad (6)$$

Using the triangle DPB and the condition that internal angles of a triangle

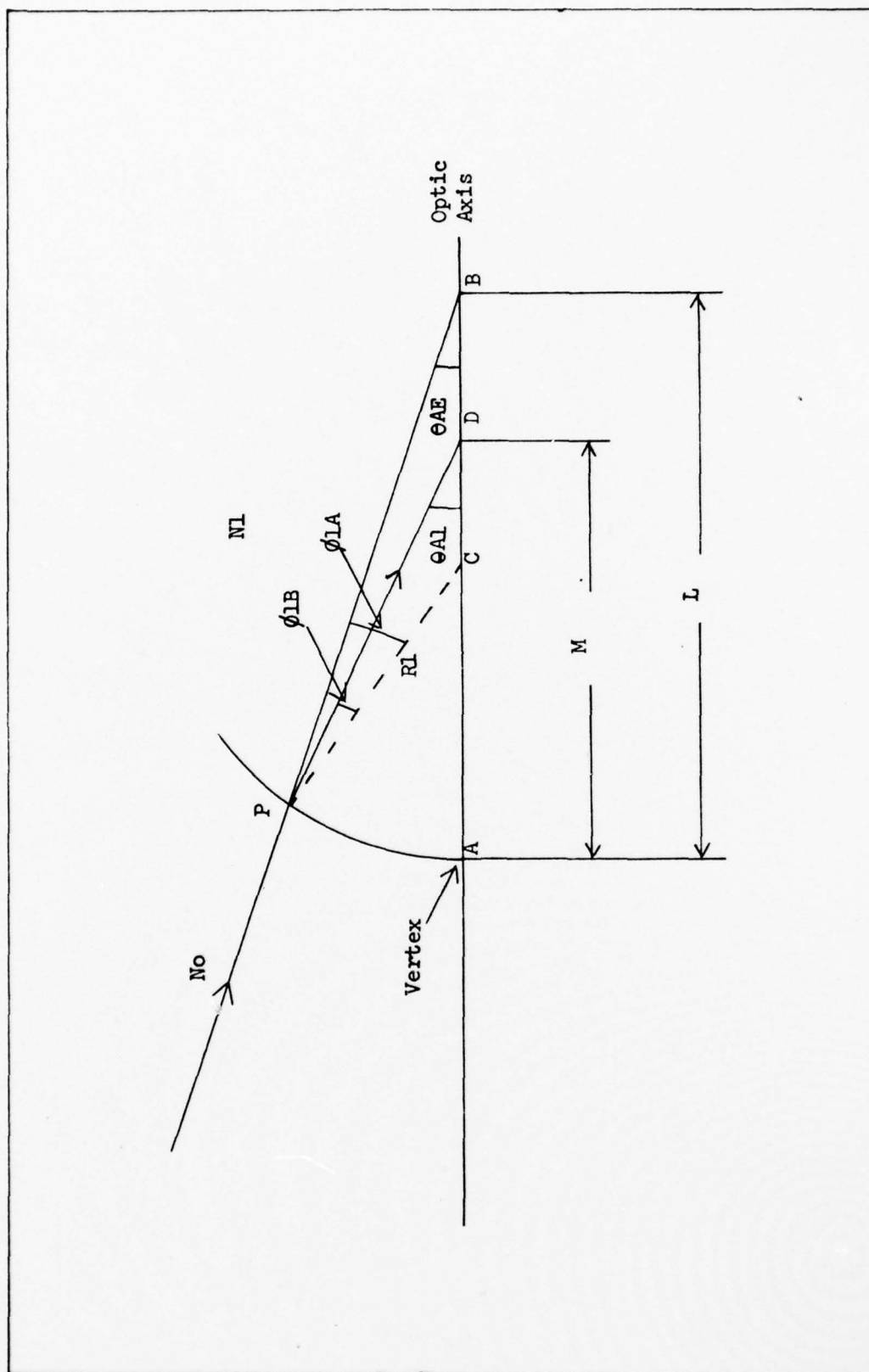


Fig. 8 - Ray Converging Toward the Optic Axis

must equal 180 degrees it is seen that

$$\theta_{A1} = \theta_{AE} + \phi_{1A} - \phi_{1B} \quad (7)$$

Also from the triangle CPD and the Law of Sines

$$\frac{M-R1}{\sin(\phi_{1b})} = \frac{R1}{\sin(\theta_{A1})} \quad (8)$$

Therefore

$$M = \frac{\sin(\phi_{1b})}{\sin(\theta_{A1})} (R1) + R1 \quad (9)$$

Where M is the distance from the vertex that the refracted ray crosses the optic axis and θ_{A1} is the angle.

B. Ray Diverging From the Optic Axis

For a ray diverging from the optic axis the method used in tracing it is from Reference 7, Section 8.3.

Figure 9 shows the ray path and notation used for this condition.

The following sign convention is followed:

The slope angles are positive when the optic axis must be rotated counterclockwise through less than 90 degrees to bring it into coincidence with the ray. The angles of incidence and refraction are positive when the radius of the surface must be rotated counterclockwise through less than 90 degrees to bring it into coincidence with the ray. Also object distances to the left of the vertex are positive and image distances to the right of the vertex are positive. Radius distance is positive if it is to the right of the vertex.

According to the sign convention stated above angles θ_{AE} , ϕ_{1A} , and ϕ_{1B} are positive while θ_{A1} is negative. Also distances L, M, and R1 are positive.

Using the Law of Sines again for triangle BPC (Fig 9)

$$\frac{L + R1}{\sin(180 - \phi_{1A})} = \frac{R1}{\sin(\theta_{AE})} \quad (10)$$

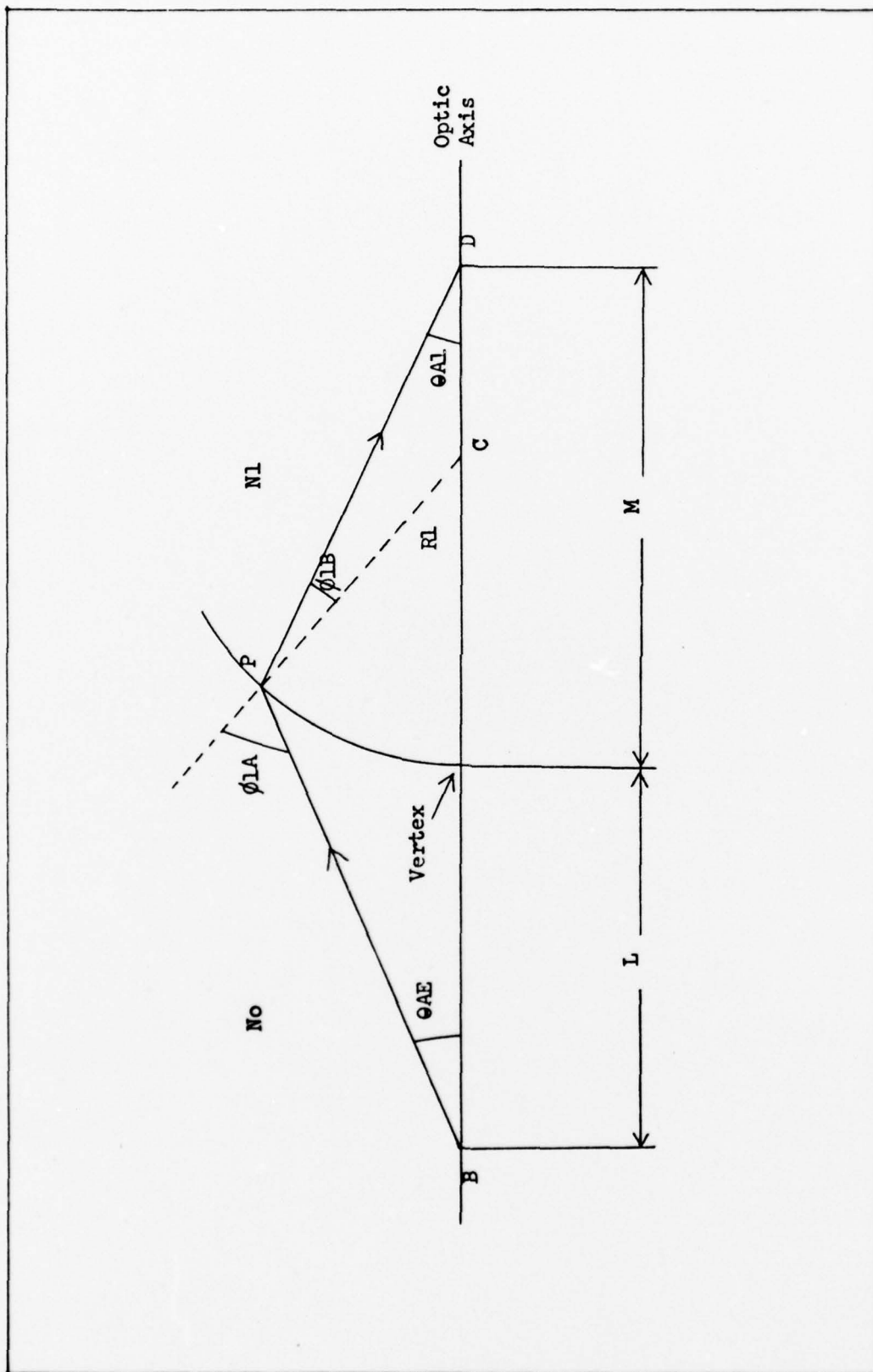


Fig. 9 - Ray Diverging From the Optic Axis

But:

$$\sin(180 - \phi_{1A}) = \sin(180)\cos(\phi_{1A}) - \cos(180)\sin(\phi_{1A}) \quad (11)$$

$$" = 0 - (-1)\sin(\phi_{1A}) \quad (12)$$

$$" = \sin(\phi_{1A}) \quad (13)$$

Substituting Eq. 13 into Eq. 10

$$\sin(\phi_{1A}) = \frac{(L+R_1)}{R_1} \sin(\theta_{AE}) \quad (14)$$

Using Snell's Law (Eq. 5) again

$$\sin(\phi_{1B}) = \frac{N_o}{N_1} \sin(\phi_{1A}) \quad (6)$$

From the triangle BPD and the sum of all interior angles of a triangle must equal 180 degrees.

$$\theta_{A1} = \phi_{1A} - \phi_{1B} - \theta_{AE} \quad (15)$$

But using the sign convention followed in this part θ_{A1} is a negative angle so

$$\theta_{A1} = \phi_{1B} + \theta_{AE} - \phi_{1A} \quad (16)$$

From triangle CPD and the Law of Sines

$$\frac{M-R_1}{\sin(\phi_{1B})} = \frac{R_1}{-\sin(\theta_{A1})} \quad (17)$$

By transforming we finally get

$$M = - \frac{\sin(\phi_{1B})}{\sin(\theta_{A1})} R_1 + R_1 \quad (18)$$

Where M is again the distance from the vertex that the refracted ray crosses the optic axis and θ_{A1} is the angle.

C. Refraction of a Ray at a Planar Surface

For a ray that is refracted at a planar (flat) surface the method used in tracing is from Reference 6, Section 4.9.

Figure 10 shows the geometry of the refraction condition and the notation used. The sign convention is the same as used in Part A (Ray

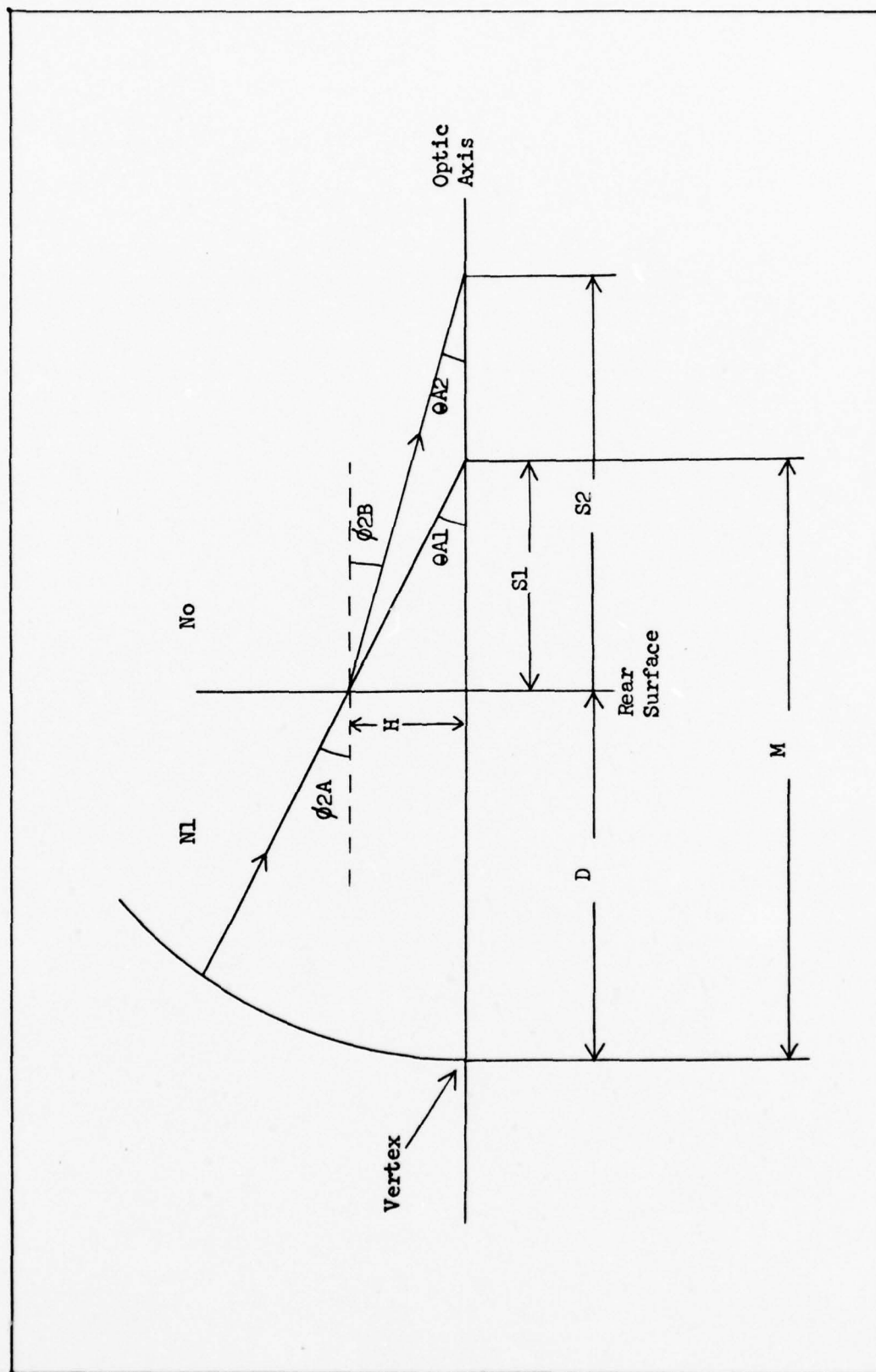


Fig. 10 - Refraction of a Ray at a Planar Surface

Converging Toward the Optic Axis). D is defined as the thickness of the lens material of index N_1 .

By geometry (Fig. 10)

$$\theta_{A1} = \phi_{2A} \quad (19)$$

Using Snell's Law (Eq. 5) again

$$\sin(\phi_{2B}) = \frac{N_1}{N_o} \sin(\phi_{2A}) \quad (20)$$

Also by geometry

$$\phi_{2B} = \theta_{A2} \quad (21)$$

And

$$S_1 = M - D \quad (22)$$

Also

$$H = (S_1) \tan(\theta_{A1}) = (S_2) \tan(\theta_{A2}) \quad (23)$$

Giving

$$S_2 = \frac{\tan(\theta_{A1})}{\tan(\theta_{A2})} (S_1) \quad (24)$$

Where S_2 is the distance from the rear surface of the lens that the refracted ray crosses the optic axis and θ_{A2} is the angle.

V. Skew Ray Analysis

When the meridional ray analysis was completed for the sun pumped laser a significant difference existed between the calculated power loss and the measured power loss. This difference made the analysis of skew ray losses by the system a necessity. A method for treating a few sample skew rays propagating through the system was therefore needed.

Reference 3, Section 5.4.1 contained a method for propagating skew rays through the system and determining their intersection points on the optical surfaces. The basic method outlined by Reference 3 uses optical direction cosines. A optical direction cosine is defined as the direction cosine of one of the cartesian components of a ray multiplied by the index of refraction of the media through which the ray is traversing. The sign of the index of refraction is positive for a ray traveling from left to right and negative for the opposite condition. Therefore, if a ray is initially traveling from left to right and reflects off a plane mirror, the index of refraction changes from positive to negative, but the direction cosine remains the same and the optical direction cosine would only change in sign.

Reflection and refraction at a spherical surface are calculated by the use of a vector form of Snell's Law. For reflection, the equation is basically the same except that the index's of refraction have the same value but different signs.

If the rays from the center of the sun have to be parallel to the optic axis to enter the Primary Mirror, then a ray coming from the extreme edge of the sun would strike the Primary Mirror with a skewness angle of 0.25 degrees. An analysis that any ray emitted from the center of the sun with a skew angle greater than 2×10^{-12} degrees, with respect to the optic axis of the sun pumped laser, will not strike the Primary Mirror.

Five skew rays were analyzed to determine their ability to propagate through the system and enter the reference circle (see Section III for a derivation of the reference circle). Two of the rays are incident on the Primary Mirror at a radial distance of 16.00 cm, about half the radial distance to the edge. Two more of the rays were incident at a radial distance of about 29.00 cm, this is close to the outer edge of the Primary Mirror. The fifth ray was incident at 22.00 cm. Of the rays incident at each point, two of the rays had a skewness angle of "0" degree with respect to the optic axis of the system, and three had a skewness angle of "+0.25" degrees. Table III shows the input parameters and the intersection points for the analysis and is computed with a 12.2 cm separation distance between the relay lens and cone lens.

TABLE III

Ray	Skewness Angle (degrees)	Primary Mirror Radial Distance (cm)	Cone Lens Radial Distance (cm)	Reference Circle Radial Distance (cm)
1.	0.00	16.21	0.30	0.44
2.	+0.25	16.21	-0.02	0.55
3.	+0.25	22.00	0.43	0.58
4.	0.00	29.20	1.42	*
5.	+0.25	29.20	1.24	*

* These rays do not enter the Condensing Cone

From Table III, it can be seen that the rays that are incident on the Primary Mirror at large radial distances do not propagate through the solar collector and are not available for pumping the laser rod.

The intersection point of the individual rays with the reference circle can be used to determine the number of bounces a ray will make before it

enters the exit opening of the Condenser Cone. The extension of the Condenser Cone theory to calculate the number of bounces for a skew ray was made by W. White in 1965 (Ref. 8). The basic method is the same as used by Williamson (Ref. 5). The extension to a three dimension analysis for calculation of the number of bounces for a skew ray involves building a theoretical reference sphere instead of a reference circle.

VI. Results and Conclusions

Results

The analysis of the through power for the solar energy collector of the sun pumped laser was made using the methods and theory outlined in Section III, Section IV and Appendix II. The basic problem was to determine the distance between the relay lens and the cone lens at which the highest percentage of available power was collected by the system. The method used to solve the problem was a meridional ray analysis of the cone optics part of the system. The cone optics part consists of the relay lens, cone lens, and condenser cone.

TABLE IV

Primary Mirror Radius Equated to
Normalized Mirror Area

Primary Mirror Radius	Entrance Pupil Image (cm)	Normalized Mirror Area
12.0"	2.35	1.00
11.5"	2.25	0.9184
11.0"	2.15	0.8402
10.5"	2.05	0.7656
10.0"	1.95	0.6944
9.5"	1.85	0.6267
9.0"	1.75	0.5625
8.5"	1.65	0.5017
8.0"	1.55	0.4444
7.5"	1.45	0.3906

Figure 11 is a graph of the power exiting the condenser cone for different distances between the relay lens and the cone lens. The analysis used to produce this graph involved meridional rays only. The peak is at 12.20 cm with the curve dropping off quickly at distances greater than 12.20 cm. The part of the curve above 10.50 cm and below 12.30 cm seems to be the optimal distance between the relay lens and the cone lens for maximum power

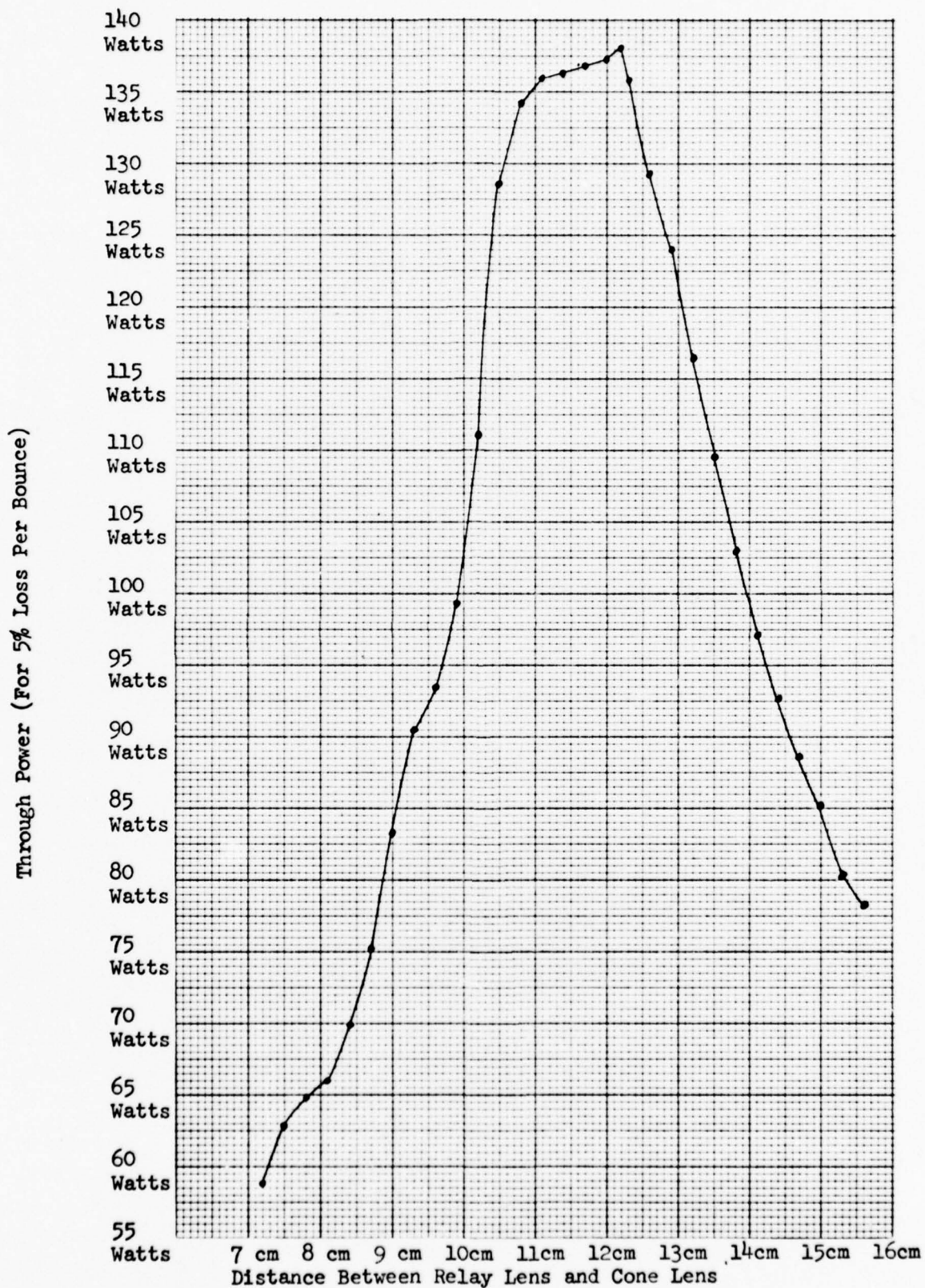


Fig. 11 - Through Power (For 5% Loss Per Bounce) vs Separation Distance

through the condenser cone.

Looking at Figure 11, the maximum power through the condenser cone is at the 12.2 cm separation distance between the relay lens and the cone. The theoretical power through the condenser cone at this point is 138 watts. The primary assumption that is used in deriving this through power is that a power loss of only five percent is realized by a ray that reflects off the condenser cone wall.

From the analysis of the meridional rays it is seen that all the rays that pass through the entrance pupil image in front of the relay lens will continue on through the system and exit the condenser cone. The rays will have from zero to five bounces in traversing the condenser cone. For a five percent power loss per bounce the remaining power in any single ray can be from 100 percent down to 77 percent. For the 200 rays used in the meridional ray analysis, all of them traversed the condenser cone and passed through the exit opening of the cone, thereby striking the end of the laser rod.

In Section V a brief skew analysis was discussed. This analysis showed that the ray incident on the primary mirror at the outer edge of the mirror do not propagate through the solar collector part of the sun pumped laser. A look at where the rays strike the relay lens shows that they cross a horizontal plane that includes the optic axis. The rays that are incident on the primary mirror at the outer edge strike the cone lens at distances greater than 0.8 cm. The condenser cone, which is against the back surface of the cone lens, only has an entrance opening of 0.8 cm and the cone lens will only refract the rays inward a small distance while it is in the lens material. Therefore, the rays striking the cone lens at a radial distance greater than 0.80 cm can be neglected

for figuring power available to pump the laser rod.

From inspection of Table III, a quick guess can be made that rays striking the primary mirror at distances greater than 25 cm are excluded because they do not enter the condenser cone for a relay lens, cone lens separation of 12.2 cm. From looking at Figure 11 again, it can be seen that good meridional ray through power is available at 10.0 cm or greater.

If it is assumed that the total power available at the output of the relay lens is 150 watts and that the rays from 25 cm on out on the primary mirror do not propagate through the system, then it is obvious that 33% of the power does not enter the condenser cone. With only 100 watts available, instead of 150 watts, and assuming that 60 watts is incident on the laser rod for a normalized primary mirror area of 1 (see Figure 2) then a transfer efficiency of 60% can be assumed for the condenser cone.

If it is again assumed that all the rays are meridional rays and that 155 watts are available, then 138 watts is collected by the condenser cone for a transfer efficiency of 89%. By looking at Table V, we can see that for a 5% loss per bounce, the lowest power a ray can have that propagates through the condenser cone is 77% of its original power. If a 15% loss per bounce is assumed for the condenser cone and the condition that all skew rays and all meridional rays from less than 25 cm radius are collected by the condenser cone then, a transfer efficiency of about 65% is realized for the average ray which makes approximately 2.5 bounces before exiting the condenser cone.

TABLE V

Power Loss for 5%, 15% and 25% Loss per Reflection

Bounces	5% Loss	15% Loss	25% Loss
0	1.0000	1.0000	1.0000
1	0.9500	0.8500	0.7500
2	0.9025	0.7225	0.5625
3	0.8573	0.6141	0.4218
4	0.8145	0.5220	0.3164
5	0.7737	0.4437	0.2373

Figures 12, 13 and 14 are graphs of the through power for different radial lengths of the primary mirror at 10.8 cm, 12.2 cm, and 13.0 cm separation between the relay and cone lens. These graphs show the through power for a point before and after the optimum point (refer to Figure 11 for the optimum point).

Using Table IV it is seen that at an entrance pupil image radius of approximately 1.75 cm (corresponding to a 9" radius primary mirror) the through power for 10.8 cm, 12.2 cm and 13.0 cm is approximately the same for a meridional ray analysis. But looking at Table III, we see that the skew rays for the outer area of the primary mirror do not propagate through the system. Therefore, it is again concluded that a closer distance between the relay lens and cone lens of approximately 10.0 to 10.5 cm would increase the through power by catching more of the skew rays while losing only a little of the meridional rays.

The last part of the sun pumped laser analysis looked at the exit angle of the rays from the condensing cone that were incident on the laser rod. An analysis was needed of the power incident on the laser rod by

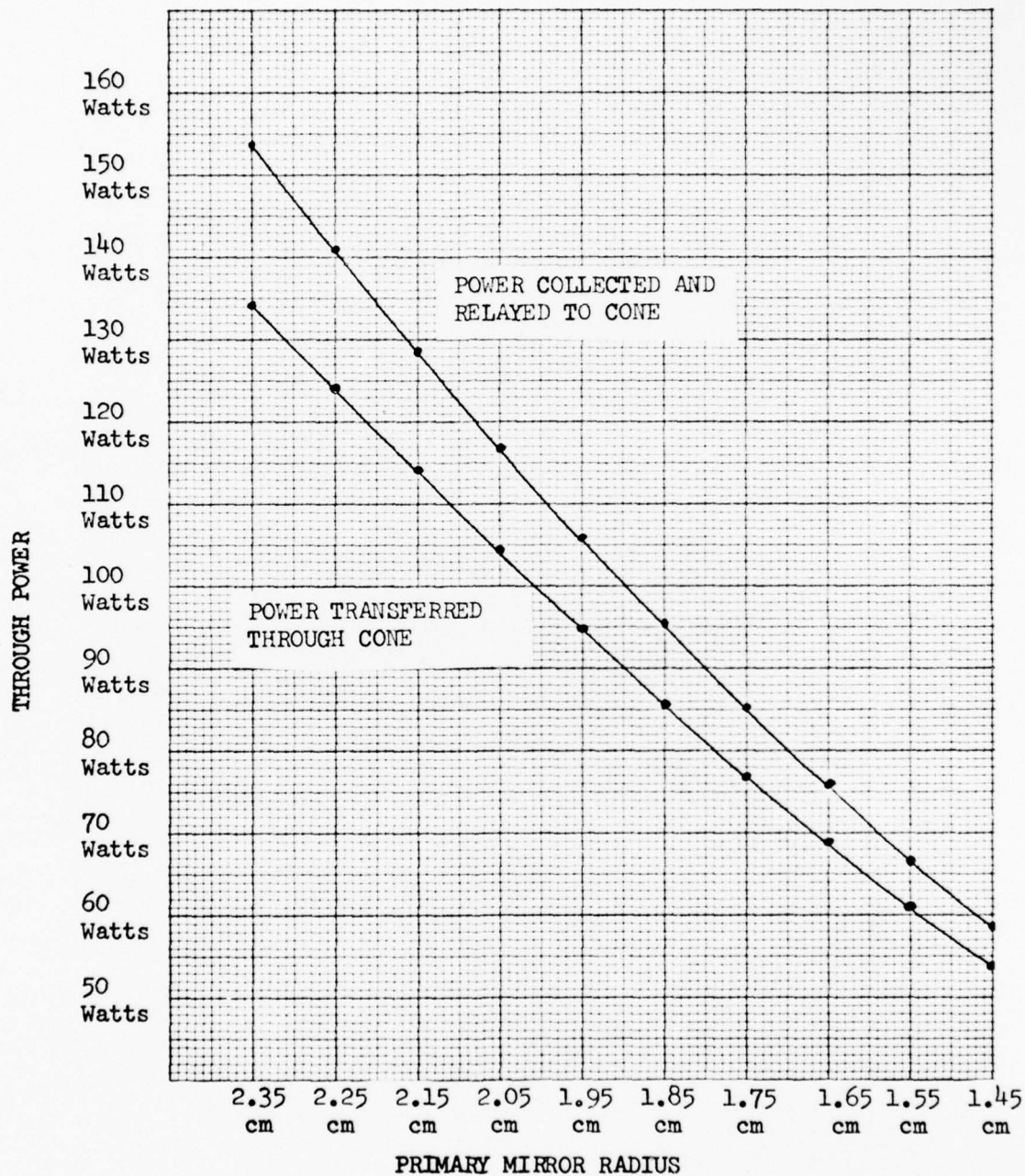


Fig. 12 - Primary Mirror Radius vs. Through Power at 10.8 cm

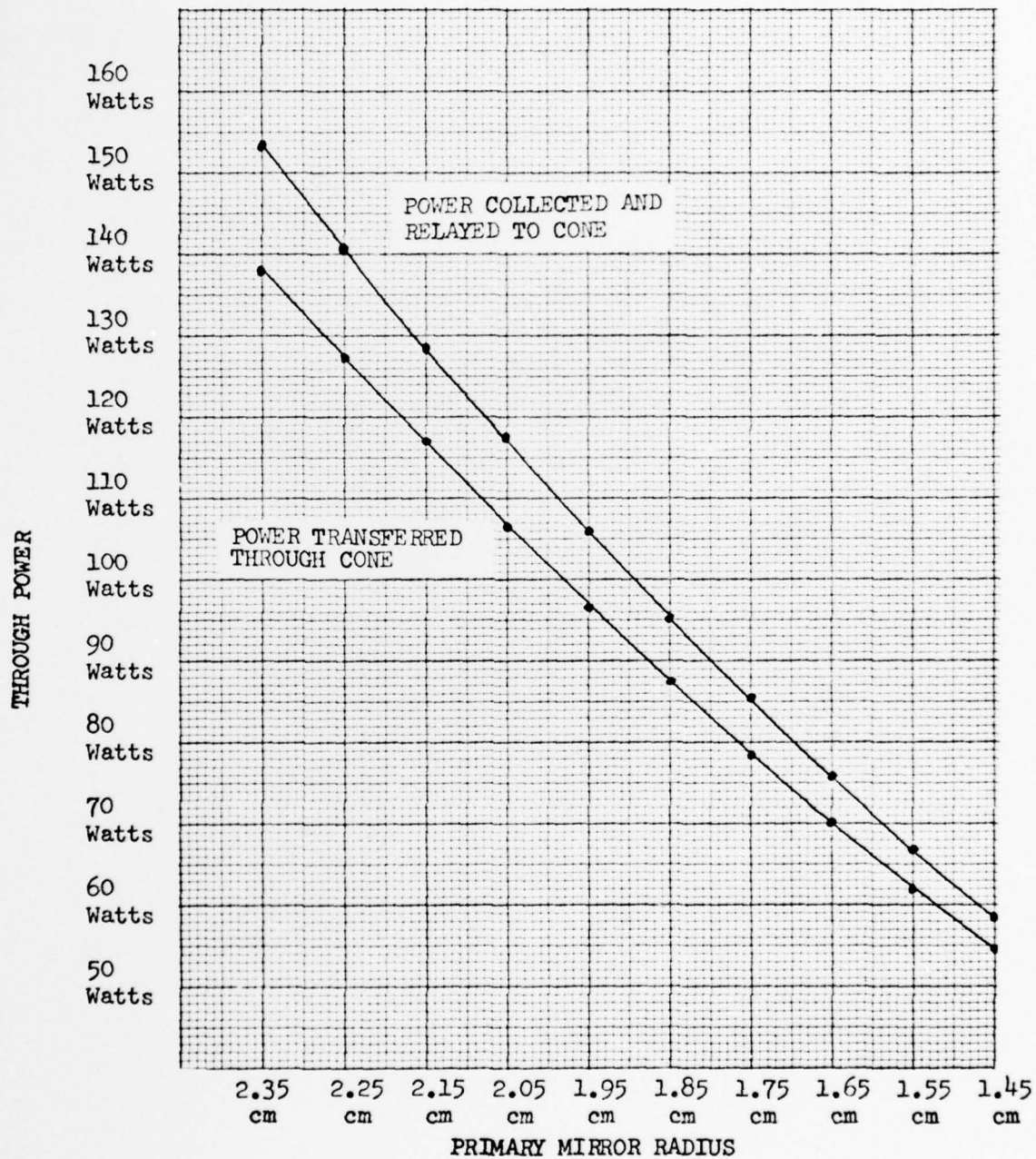


Fig. 13 - Primary Mirror Radius vs. Through Power at 12.2 cm

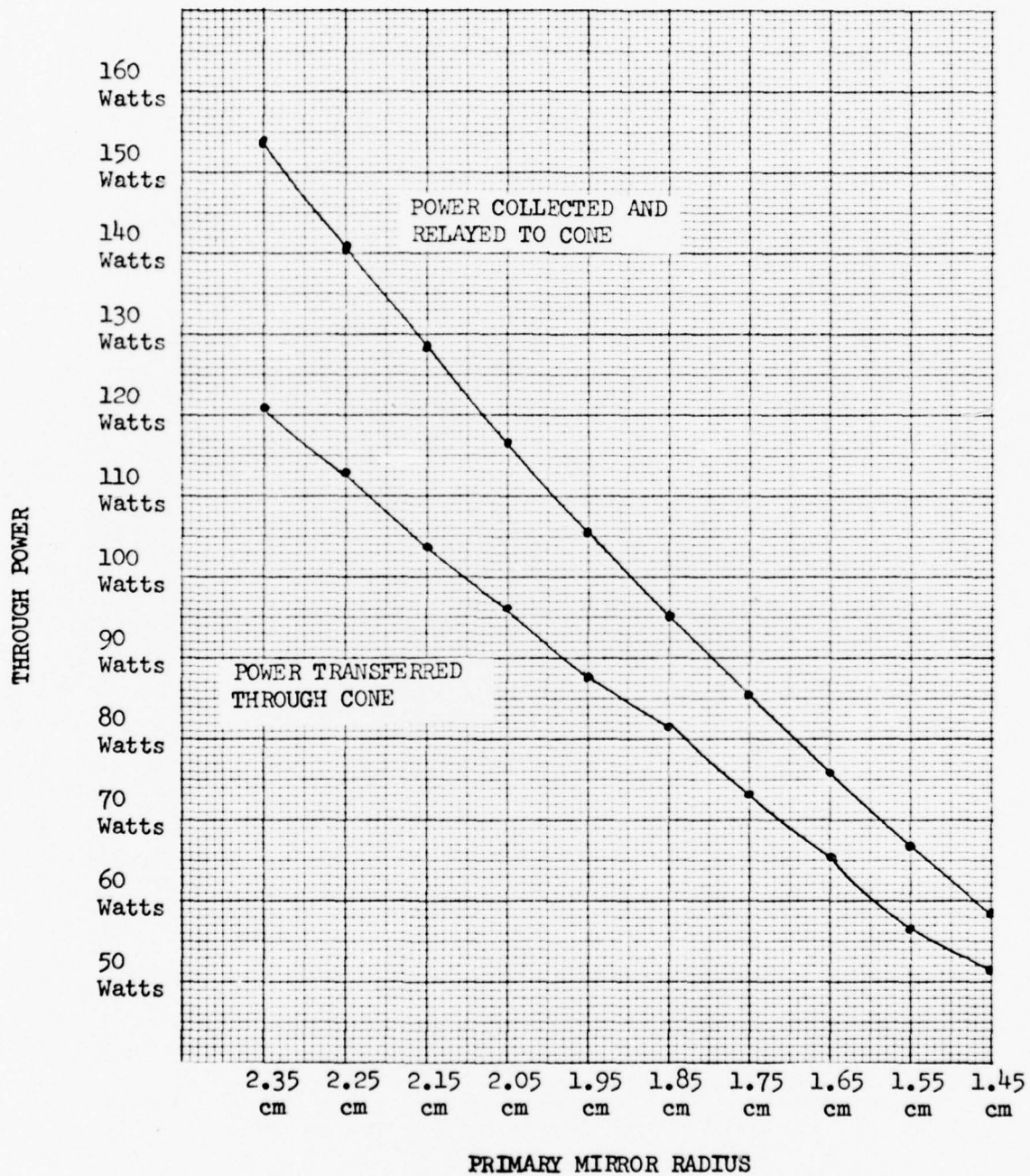


Fig. 14 - Primary Mirror Radius vs. Through Power at 13.0 cm

azimuth zone. This information would be used to determine the thickness of an AR coating on the end of the laser rod that received the solar energy. Appendix C is a derivation of how the "Azimuth Zone Power Factors" were calculated. Table VI shows the "Azimuth Zone Power Factors" for 9.9 cm, 12.2 cm and 13.2 cm, while Table VII is a listing for distances between 9.0 cm to 13.8 cm separation between the relay lens and the cone lens. "Azimuth Zone Power Factors" is a weighting of each azimuth zone by the incident power.

TABLE VI

Azimuth Zone Power Factors

Entrance Angle (degrees)	9.9 cm Separation	12.2 cm Separation	13.2 cm Separation
0-10	0.04198	0.05200	0.05532
10-20	0.07984	0.13404	0.15056
20-30	0.05544	0.08073	0.09028
30-40	0.15158	0.29706	0.25216
40-50	0.08307	0.08664	0.13664
50-60	0.11081	0.17600	0.04063
60-70	0.09846	0.03730	0.00325
70-80	0.00	0.00	0.00
80-90	0.00	0.00	0.00

Note - Angles are measured from the normal, therefore 0 degrees is normal to the end of the laser rod.

Conclusions

1. A skew ray problem does exist and needs to be investigated and appropriate changes made in the system.
2. If the skew ray problem cannot be investigated, then the distance between the relay lens and cone lens should be adjusted for maximum output by placing a power meter at the exit of the condenser cone and varying the distance.

3. The reflective loss per bounce for the condenser cone should be checked and a material analysis accomplished to determine which material would give the least loss at the solar energy wavelengths that are being used to pump the Nd:YAG rod.

Bibliography

1. Simpson, G. R. "Sun Pumped Laser Operation." Applied Optics, 1: 783 (1964)
2. Young, C. G. "A Sun Pumped CW One-Watt Laser." Applied Optics, 5: 993 (1966)
3. MIL-HDBK-141. Optical Design. Washington: Department of Defense, October 1962.
4. AFAL-TR-72-310. Sun Pumped Laser. Washington: Department of the Air Force, November 1972.
5. Willaimson, D. E. "Cone Channel Condenser Optics." Journal of the Optical Society of America, 42: 712-715 (October 1952)
6. Born, M. and E. Wolf. Principles of Optics (Fifth Edition). New York: Pergamon Press, 1975.
7. Jenkins, F. A. and H. E. White. Fundamentals of Optics (Third Edition). New York: McGraw-Hill Book Co., 1957.
8. White, W. "Cone Channel Optics." Infrared Physics, 5: 179-185 (1965)

Appendix A

Entrance Pupil Calculation

A calculation of the entrance pupil of the solar collector was necessary to determine the limiting condition on a ray going through the system. The following method was used in determining the Aperture Stop and Entrance Pupil:

- a. Image all the elements into object space.
- b. Find the angle subtended by each element at the on-axis position of the object (i.e. the sun).
- c. The element with the smallest angle is the aperture stop and its image is the entrance pupil.

Elements looked at in the calculation of the entrance pupil:

- a. Primary Mirror
- b. Secondary Mirror
- c. Field Lens
- d. Two inch aperture in Primary Mirror
- e. Relay Lens
- f. Cone Lens
- g. Reference Circle

All the elements of the system were imaged into object space and their image sizes were determined. Then using an average solar distance of 1.496×10^{13} cm. the angle at the object was found. Following is Table VII which lists all the elements, the image distance from the Primary Mirror and the angle subtended.

TABLE VII

System Elements and Parameters Used in Entrance Pupil Calculation

1. Primary Mirror*	Image Distance	= 0 cm
	Image Radius	= 30.48 cm
	Angle Subtended	= 2.03743×10^{-12} radians
2. Secondary Mirror	Image Distance	= 983 cm
	Image Radius	= 45.0 cm
	Angle Subtended	= 3.0080×10^{-12} radians
3. Field Lens	Image Distance	= 14,078.6 cm
	Image Radius	= 80.1 cm
	Angle Subtended	= 5.3542×10^{-12} radians
4. Aperture in Primary (2")	Image Distance	= -10,132.66 cm
	Image Radius	= 77.5 cm
	Angle Subtended	= 5.1804×10^{-12} radians
5. Relay Lens	Image Distance	= 2,247.5 cm
	Image Radius	= 66.89 cm
	Angle Subtended	= 4.4712×10^{-12} radians
6. Cone Lens	Image Distance	= 936,560 cm
	Image Radius	= 4,211.5 cm
	Angle Subtended	= 2.8×10^{-9} radians
7. Reference Circle	Image Distance	= 145 cm
	Image Radius	= 30.84 cm
	Angle Subtended	= 2.0614×10^{-12} radians

* The Primary Mirror subtends the smallest angle at the Sun and therefore is the aperture stop and the entrance pupil.

Appendix B

Power "Weight Factor" Derivation for Radial Zones

In computing the through power for the solar collector a method of determining the power in each ray is necessary. The incident solar radiation on the Primary Mirror is a function of the presented area. Therefore, when determining the power in a ray traversing the system, a weighting factor is needed that corresponds to the presented area of the Primary Mirror segment which the ray represents.

The Snell's Law ray trace of the system started with a solar image at the Field Lens and an entrance pupil image at the Relay Lens. A method of starting the rays from the solar image and passing them through the entrance pupil image with a weighting factor corresponding to the normalized area of the solar image radial zone from which the ray started times the normalized area of the entrance pupil radial zone through which the ray passed seemed best.

Since the solar collector of the sun pumped laser is symmetrical about the optic axis, only rays coming from the top half of the solar image were needed (Fig.15). These rays were passed through the different zones of the entrance pupil image and propagated on through the system. If the ray entered the reference circle the loss due to bounces was multiplied by the weight factor. In doing the analysis, two hundred rays were run through the system with twenty rays coming from each solar image radial zone. This put one ray from each solar image radial zone through each of the entrance pupil radial zones.

The final power through the system is then determined by multiplying the normalized weight factor for each ray by the power available. This is then adjusted by the loss factor due to bounces. The power for all the

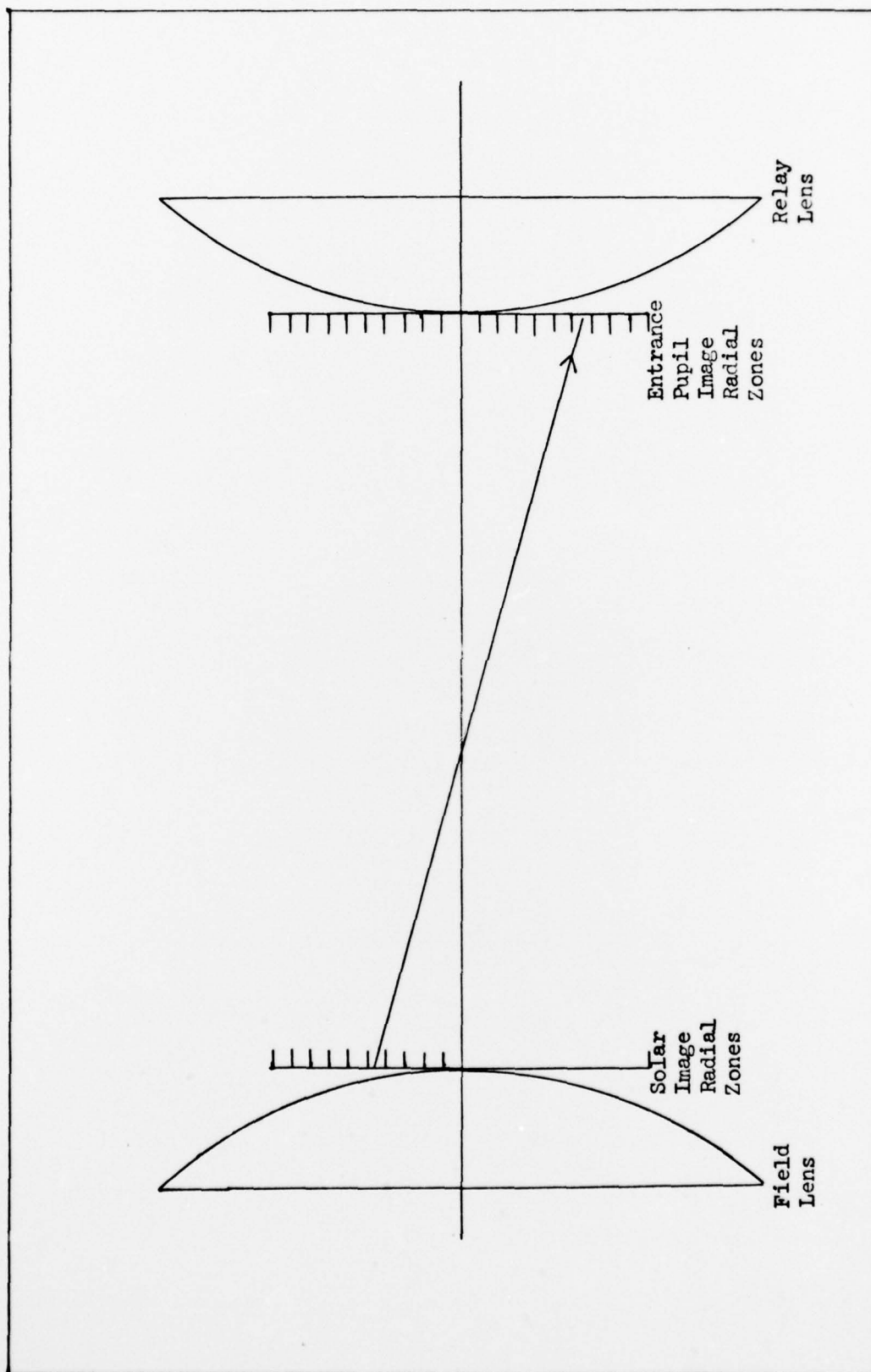


Fig. 15 - Solar Image and Entrance Pupil Image Radial Zones

rays exiting the system at the exit opening of the condenser cone are then summed. This sum is the final power out of the solar collector for a meridional ray analysis.

The solar image was 2.80 cm radius and it was divided into ten radial zones each of 0.38 cm radius. The total area of the solar image was

$$A = r^2 \quad (26)$$

$$A = 24.63 \text{ cm}^2 \quad (27)$$

This was the normalizing factor used for the solar image radial zones.

The entrance pupil image has a 2.35 cm radius and a normalizing area of 17.34 cm^2 . In the following example a ray from the fifth solar image radial zone is passed through the third entrance pupil image radial zone and the normalized area is calculated.

The area of the Nth zone can be calculated by multiplying the radial zone size (0.28 cm) by N and finding that area.

$$A1 = (N \times 0.28)^2 \quad (28)$$

Then find the (N-1)th zone area

$$A2 = (N-1)^2 \times (0.28)^2 \quad (29)$$

Then subtract A2 from A1

$$A2 - A1 = (6.15 - 3.94) \text{ cm}^2 \quad (30)$$

$$A2 - A1 = 2.21 \text{ cm}^2 \quad (31)$$

Then the area can be normalized by dividing by the total area of the solar image (Eq 27)

$$A (\text{normalized}) = 2.21/24.63 \quad (32)$$

$$A (\text{normalized}) = 0.090 \quad (33)$$

Appendix C

Derivation of the "Azimuth Zone Power Factors" Used to Calculate the Power Distribution Out of the Condensing Cone by Exit Angle

The analysis of the through power by exit angle would be an easy task if the Condenser Cone were not in the system. The Condenser Cone makes the portion of the energy not directly entering the laser rod reflect one or more times before reaching the rod. Therefore, the angle that the reflected energy makes on entering the rod is a function of the initial angle it makes with the optic axis, the number of reflections before it enters the rod and the sign of the angle the ray makes when leaving the rear surface of the Cone Lens (i.e. whether or not the ray is converging towards the optic axis or diverging away from the optic axis).

An analysis of how a ray making one bounce and enters the laser rod would show the relationship between the three factors contributing to the exit angle calculation.

Figure 16 shows the exit opening of the Condenser Cone and the first rotation of the cone about one of its reflecting surfaces. Ray \bar{A} enters the reference circle after only one bounce and is coming from the optic axis while ray \bar{B} also enters the reference circle after only one bounce but is converging toward the optic axis someplace beyond the vertex. Ray \bar{C} enters the reference circle without any reflections. The angle at which ray \bar{C} enters the laser is easy to calculate. Since θ_{3C} (the angle the ray makes with the optic axis) is known and the exit opening is normal to the optic axis, a right triangle can be formed from the exit opening, the optic axis and the ray. With one angle equal to 90 and θ_{3C} known, the exit angle of ray \bar{C} can be calculated from

$$\text{Exit Angle} = 90 - \theta_{3C} \quad (34)$$

The angle that ray \bar{A} makes when entering the reference circle can be determined by knowing the full cone angle and the angle the ray makes

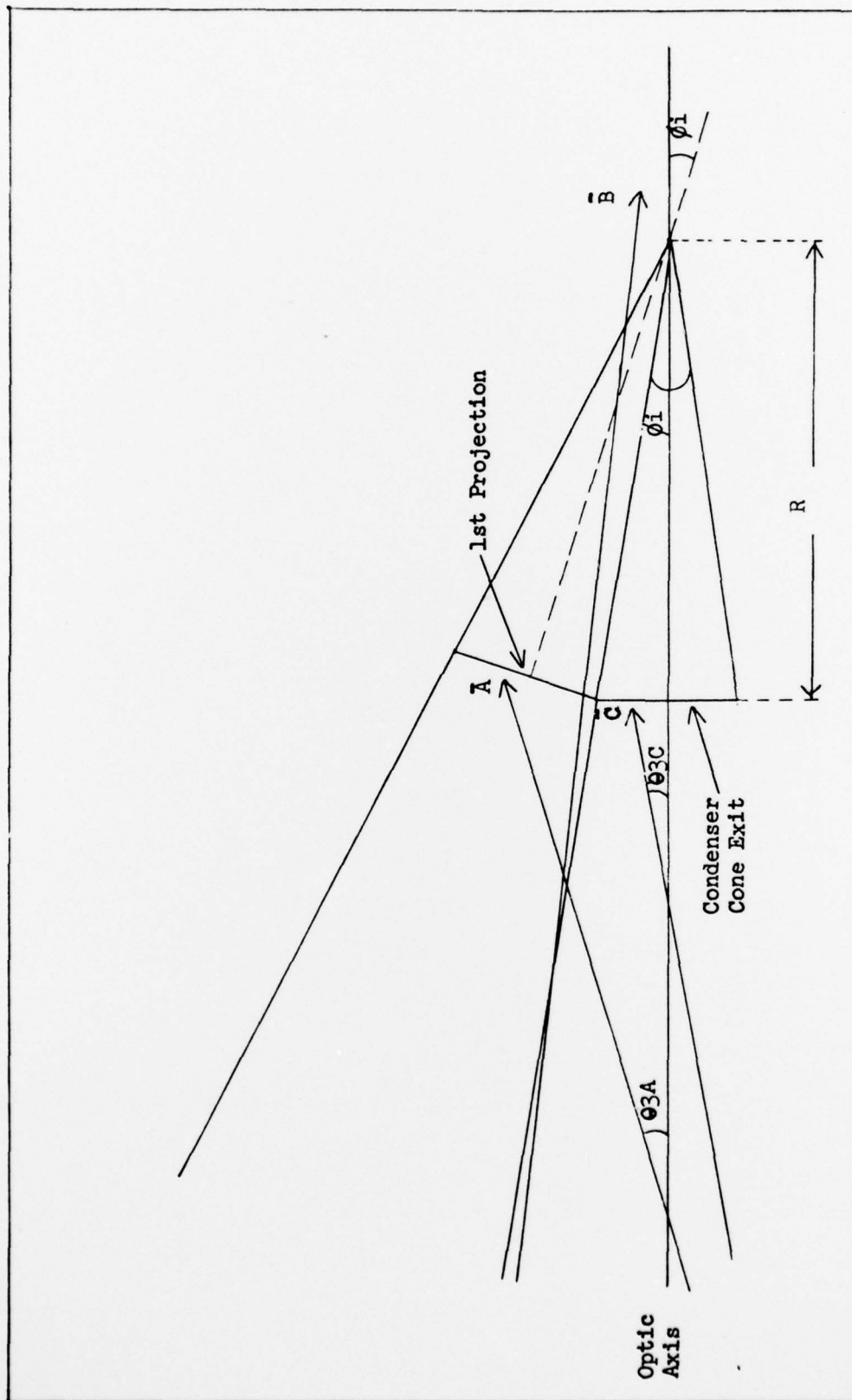


Fig. 16 - Ray Intersect Angles for Condenser Cone Exit

with the optic axis (θ_{3A}). The exit opening of the reference circle for a single bounce ray has been inclined away from the exit opening of the zero bounce by an angle equal to the full cone angle (ϕ_i) (for this cone that is 17.7 degrees). Therefore, the exit angle equation of the one bounce zone would be equal to the exit angle of the zero bounce zone minus the inclination angle. The equation is

$$\text{Exit Angle (one bounce zone)} = 90 - \phi_i - \theta_{3A} \quad (35)$$

For rays entering the reference circle with more than one bounce and coming from the optic axis the equation is basically the same with the angle ϕ_i being a function of the number of bounces (N). The exit angle equation for the Nth bounce zone is then

$$\text{Exit Angle (Nth bounce zone)} = 90 - N\phi_i - \theta_{3A} \quad (36)$$

The angle ray " \bar{B} " makes when crossing the optic axis at a point beyond the vertex will be called θ_{3B} . The reference circle will be inclined with respect to ray " \bar{B} " in the opposite direction, it is inclined with respect to ray " \bar{A} ". Looking at Figure 17 the angle ϕ_i is the inclination angle of the reference circle zone and ϕ_A is the third angle in the right triangle and is equal to

$$\phi_A = 90 - \theta_{3B} \quad (37)$$

The exit angle ϕ_E is then found from

$$\phi_E = 180 - \phi_i - \phi_A \quad (38)$$

On substituting ϕ_A the equation becomes

$$\phi_E = 180 - \phi_i - (90 - \theta_{3B}) \quad (39)$$

or

$$\phi_E = 90 - \phi_i + \theta_{3B} \quad (40)$$

where ϕ_E is the exit angle.

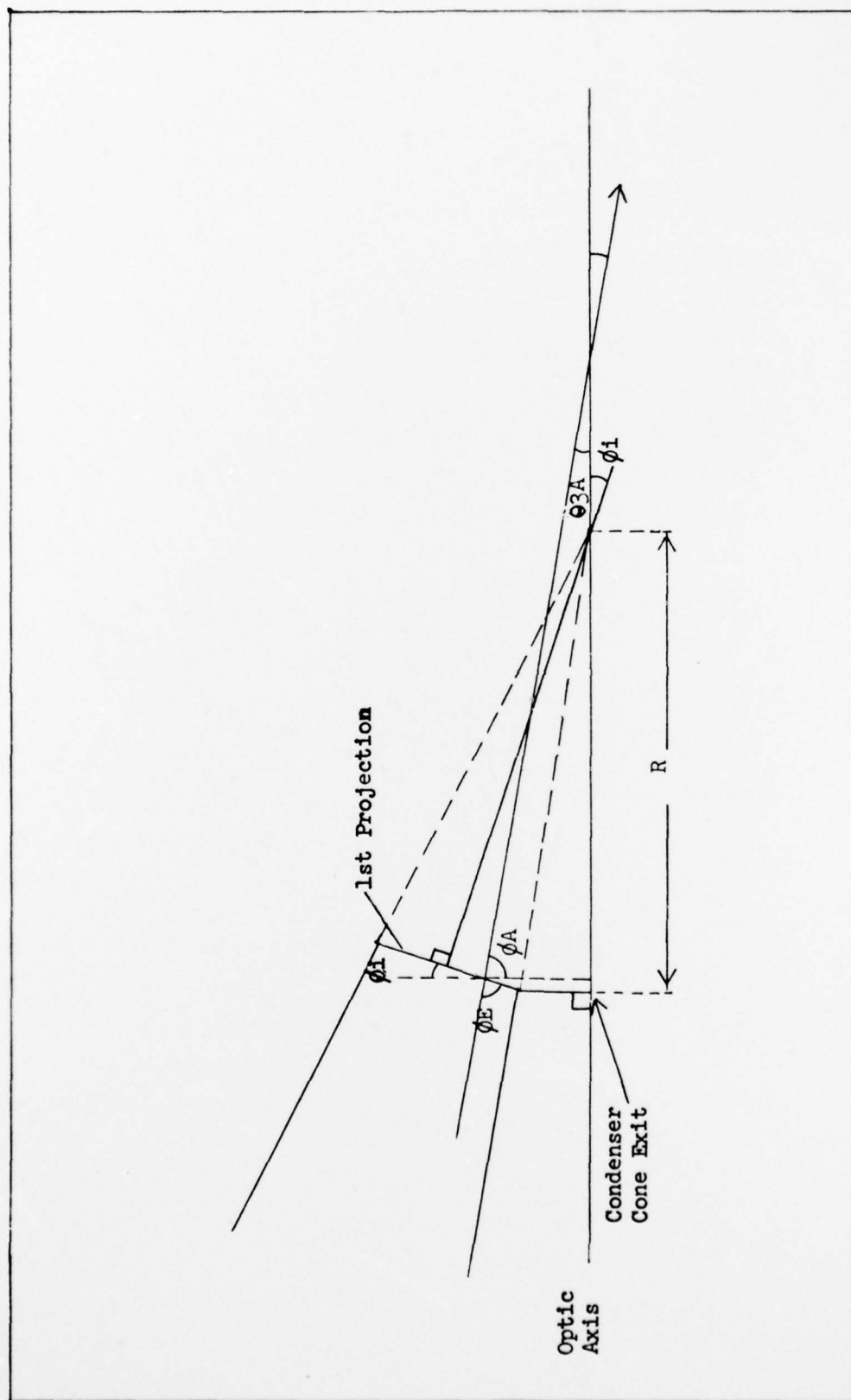


Fig. 17 - Ray Intersect Angle for Converging Ray (\bar{B})

If the ray enters the Nth bounce zone and is converging towards the optic axis a expansion of the equation shows that for the Nth bounce zone we get the following equation:

$$\text{Exit angle (Nth bounce zone)} = 90 - N\phi_i + \phi_{3B} \quad (41)$$

Following is a table of the "Azimuth Zone Power Factors" for different distances between the relay lens and the cone lens.

TABLE VIII

Azimuth Zone Power Factors for Different Distance
Between the Relay Lens and the Cone Lens

Distance 9.0 cm Az Zone Power Factors	Distance 9.3 cm Az Zone Power Factors	Distance 9.6 cm Az Zone Power Factors
00-10 = 0.04145	00-10 = 0.04145	00-10 = 0.04181
10-20 = 0.06258	10-20 = 0.06990	10-20 = 0.07765
20-30 = 0.05483	20-30 = 0.05644	20-30 = 0.05232
30-40 = 0.08228	30-40 = 0.09812	30-40 = 0.13191
40-50 = 0.09492	40-50 = 0.08760	40-50 = 0.08464
50-60 = 0.06272	50-60 = 0.06877	50-60 = 0.05234
60-70 = 0.05045	60-70 = 0.05905	60-70 = 0.06794
70-80 = 0.03279	70-80 = 0.04372	70-80 = 0.05060
80-90 = 0.03987	80-90 = 0.04153	80-90 = 0.02492
Distance 9.9 cm Az Zone Power Factors	Distance 10.2 cm Az Zone Power Factors	Distance 10.5 cm Az Zone Power Factors
00-10 = 0.04198	00-10 = 0.04198	00-10 = 0.04173
10-20 = 0.07984	10-20 = 0.08329	10-20 = 0.09065
20-30 = 0.05544	20-30 = 0.05362	20-30 = 0.06293
30-40 = 0.15158	30-40 = 0.17376	30-40 = 0.16863
40-50 = 0.08307	40-50 = 0.07511	40-50 = 0.08215
50-60 = 0.11081	50-60 = 0.13622	50-60 = 0.17666
60-70 = 0.09846	60-70 = 0.06541	60-70 = 0.04693
70-80 = 0.0	70-80 = 0.04157	70-80 = 0.10787
80-90 = 0.0	80-90 = 0.02398	80-90 = 0.02785
Distance 10.8 cm Az Zone Power Factors	Distance 11.1 cm Az Zone Power Factors	Distance 11.4 cm Az Zone Power Factors
00-10 = 0.04248	00-10 = 0.04333	00-10 = 0.04443
10-20 = 0.10615	10-20 = 0.11816	10-20 = 0.11955
20-30 = 0.05930	20-30 = 0.06338	20-30 = 0.06674
30-40 = 0.21099	30-40 = 0.21997	30-40 = 0.22967
40-50 = 0.08824	40-50 = 0.07901	40-50 = 0.07138
50-60 = 0.15773	50-60 = 0.19593	50-60 = 0.20763
60-70 = 0.04523	60-70 = 0.07873	60-70 = 0.07218
70-80 = 0.11060	70-80 = 0.05212	70-80 = 0.04153
80-90 = 0.01980	80-90 = 0.0	80-90 = 0.0

Distance 11.7 cm
Az Zone Power Factors

00-10 = 0.04443
10-20 = 0.12400
20-30 = 0.06518
30-40 = 0.26064
40-50 = 0.07178
50-60 = 0.19206
60-70 = 0.06905
70-80 = 0.02931
80-90 = 0.0

Distance 12.0 cm
Az Zone Power Factors

00-10 = 0.0493
10-20 = 0.12443
20-30 = 0.08312
30-40 = 0.28176
40-50 = 0.06977
50-60 = 0.18289
60-70 = 0.05440
70-80 = 0.01384
80-90 = 0.0

Distance 12.2 cm
Az Zone Power Factors

00-10 = 0.05200
10-20 = 0.13404
20-30 = 0.08073
30-40 = 0.29706
40-50 = 0.08664
50-60 = 0.17600
60-70 = 0.03730
70-80 = 0.0
80-90 = 0.0

Distance 12.3 cm
Az Zone Power Factors

00-10 = 0.05655
10-20 = 0.12969
20-30 = 0.08073
30-40 = 0.30307
40-50 = 0.08989
50-60 = 0.16315
60-70 = 0.02671
70-80 = 0.0
80-90 = 0.0

Distance 12.6 cm
Az Zone Power Factors

00-10 = 0.05655
10-20 = 0.15251
20-30 = 0.08059
30-40 = 0.26065
40-50 = 0.11239
50-60 = 0.13235
60-70 = 0.01368
70-80 = 0.0
80-90 = 0.0

Distance 12.9 cm
Az Zone Power Factors

00-10 = 0.0612
10-20 = 0.15693
20-30 = 0.08192
30-40 = 0.25998
40-50 = 0.13364
50-60 = 0.07558
60-70 = 0.00781
70-80 = 0.0
80-90 = 0.0

Distance 13.2 cm
Az Zone Power Factors

00-10 = 0.05532
10-20 = 0.15056
20-30 = 0.09028
30-40 = 0.25216
40-50 = 0.13664
50-60 = 0.04063
60-70 = 0.00325
70-80 = 0.0
80-90 = 0.0

Distance 13.5 cm
Az Zone Power Factors

00-10 = 0.06054
10-20 = 0.12824
20-30 = 0.08609
30-40 = 0.23979
40-50 = 0.14007
50-60 = 0.03086
60-70 = 0.0
70-80 = 0.0
80-90 = 0.0

Distance 13.8 cm
Az Zone Power Factors

00-10 = 0.06377
10-20 = 0.12491
20-30 = 0.010704
30-40 = 0.19217
40-50 = 0.15608
50-60 = 0.0
60-70 = 0.0
70-80 = 0.0
80-90 = 0.0

Note - All angles are measured with respect to the normal therefore,
0 degrees is normal to the surface of the laser rod.

VITA

Perry Michael Towles was born on 4 March 1943 in Port of Spain, Trinidad, British West Indies. He entered the Air Force on 8 February 1961. In June 1970 he was accepted into the Airman's Education and Commissioning Program (AECP) and attended the University of Arizona. Upon graduation in June 1972 with a Bachelor's of Science in Physics, he attended OTS and was commissioned in September 1972. He then worked at the Air Force Armament Laboratory, Eglin AFB, Florida in Target Vulnerability until entering the School of Engineering, Air Force Institute of Technology in June 1975.

Permanent address: 1542 Roy Drive

West Palm Beach, Florida 33406

UNCLASSIFIED

SECURITY CLASSIFICATION OF THIS PAGE (When Data Entered)

REPORT DOCUMENTATION PAGE		READ INSTRUCTIONS BEFORE COMPLETING FORM
1. REPORT NUMBER GEP/PH/76-11	2. GOVT ACCESSION NO.	3. RECIPIENT'S CATALOG NUMBER
4. TITLE (and Subtitle) ANALYSIS OF THE SUN PUMPED LASER CONE OPTICS		5. TYPE OF REPORT & PERIOD COVERED MS Thesis
7. AUTHOR(s) PERRY M. TOWLES CAPT		6. PERFORMING ORG. REPORT NUMBER
9. PERFORMING ORGANIZATION NAME AND ADDRESS Air Force Institute of Technology (AFIT-EN) Wright-Patterson AFB, Ohio 45433		8. CONTRACT OR GRANT NUMBER(s)
11. CONTROLLING OFFICE NAME AND ADDRESS Space and Missiles System Organization(SKA) Los Angeles AFS, California 90009		10. PROGRAM ELEMENT, PROJECT, TASK AREA & WORK UNIT NUMBERS
14. MONITORING AGENCY NAME & ADDRESS (if different from Controlling Office)		12. REPORT DATE September, 1976
		13. NUMBER OF PAGES 59
		15. SECURITY CLASS. (of this report) UNCLASSIFIED
		15a. DECLASSIFICATION DOWNGRADING SCHEDULE
16. DISTRIBUTION STATEMENT (of this Report) Approved for public release; distribution unlimited		
17. DISTRIBUTION STATEMENT (of the abstract entered in Block 20, if different from Report)		
18. SUPPLEMENTARY NOTES Approved for public release; IAW AFR 190-17 <i>Jerral F. Guess</i> JERRAL F. GUESS, Captain, USAF Director of Information		
19. KEY WORDS (Continue on reverse side if necessary and identify by block number) Optics Laser		
20. ABSTRACT (Continue on reverse side if necessary and identify by block number) A meridional ray analysis is accomplished on the solar energy collector part of a sun pumped laser. A Gaussian approximation is completed and shows a solar image 0.57 inches in diameter is located 3.81 cm from the end of the laser rod. The image is inside the laser cavity. The peak in meridional ray through power is found when there is a separation distance of 12.2 cm between the relay lens and the cone lens, condensing cone element.		

DD FORM 1 JAN 73 1473

EDITION OF 1 NOV 65 IS OBSOLETE

UNCLASSIFIED

SECURITY CLASSIFICATION OF THIS PAGE (When Data Entered)

UNCLASSIFIED

SECURITY CLASSIFICATION OF THIS PAGE(When Data Entered)

For 200 watts available at the primary mirror of the Cassegrainian System, it is found that only about 150 watts is furnished to the cone lens for through put. Only about 66% of the available 150 watts is collected by the cone lens and channelled to the laser rod by the condensing cone.

The last is found by a skew ray analysis of some rays coming from the outer radial part of the primary mirror. These rays are traversing the system all the way to the cone lens, but are diverging before entering the lens and therefore not being collected by the condenser cone.

An analysis is made of the exit angle of the power traversing the condenser cone. The analysis was made so that an AR coating of the appropriate material and thickness could be put on the laser rod for maximum collection of the solar energy wavelengths used in pumping the Nd:YAG laser rod.

UNCLASSIFIED

SECURITY CLASSIFICATION OF THIS PAGE(When Data Entered)